

Montclair State University

Montclair State University Digital Commons

Theses, Dissertations and Culminating Projects

5-2014

Geochemistry and Protolith Determination of the Hypersthene-Quartz-Oligoclase Gneiss from the Hudson Highlands, New York

Kathleen Miller

Follow this and additional works at: <https://digitalcommons.montclair.edu/etd>



Part of the [Environmental Sciences Commons](#)

MONTCLAIR STATE UNIVERSITY

Geochemistry and Protolith Determination of the Hypersthene-quartz-oligoclase Gneiss from the Hudson Highlands, New York

By

Kathleen Miller

A Master's Thesis Submitted to the Faculty of

Montclair State University

In Partial Fulfillment of the Requirements

For a Degree of


Master of Science

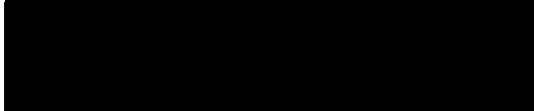
May 2014

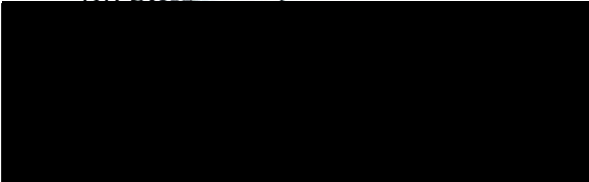
College College of Science and Mathematics

Department Earth and Environmental Studies

Thesis Committee:


Dr. Matthew Goring


Dr. Stefanie Brachfeld


Dr. Michael Krueger

ABSTRACT

The hypersthene-quartz-oligoclase gneiss of the Hudson Highlands, NY mapped by Dodd (1965) has been of unknown origin due to complex field relations resulting from metamorphism and deformation during the Ottawaan Orogeny, and a lack of geochemical data. The rock types in the Hudson Highlands and New Jersey Highlands are grouped into four general categories: metasedimentary gneisses, metaigneous gneisses, quartzofeldspathic gneisses, and syn-tectonic intrusive granitoid rocks (Dodd, 1965). Major element geochemistry and mineralogy of the Losee Metamorphic Suite of the physically contiguous New Jersey Highlands is similar to that of the hypersthene-quartz-oligoclase gneiss of the Hudson Highlands. Based on the high Al_2O_3 , CaO, $\text{Na}_2\text{O}/\text{K}_2\text{O}$ ratios, and mineralogical similarities between these units suggests an igneous protolith is likely the source of the hypersthene-quartz-oligoclase gneiss rather than a sedimentary protolith. Geochemical diagrams reveal that the hypersthene-quartz-oligoclase gneiss is of calc-alkaline affinity, ranges in composition from basalt to dacite, and is indicative of a convergent margin tectonic setting. Trace element data plotted on multi-element diagrams and Rare Earth Element (REE) plots are indicative of a continental arc subduction zone setting for the hypersthene-quartz-oligoclase gneiss. Variable heavy rare earth element (HREE) enrichment and depletion in the samples indicates that crystal fractionation from a single parent magma was unlikely. Rather, the REE patterns suggest that the magmas that formed the hypersthene-quartz-oligoclase gneiss were generated from different source rocks (e.g. upper mantle and lower mafic continental crust) and at varied depths in a continental arc setting (Winter, 2010).

GEOCHEMISTRY AND PROTOLITH INTERPRETATION OF THE
HYPERSTHENE-QUARTZ-OLIGOCLASE GNEISS FROM THE HUDSON
HIGHLANDS, NEW YORK.

Kathleen Miller

Submitted in partial fulfillment of the requirements for
the degree of Masters of Science

Department of Earth and Environmental Studies

Montclair State University

Montclair, NJ

May 2014

Copyright © 2014 by Kathleen Miller. All rights reserved.

ACKNOWLEDGEMENTS

First, I would like to thank Dr. Matthew Gorrington for all of his guidance throughout this project but most especially for going through pages upon pages of Excel spreadsheets. I would also like to thank my committee members, Dr. Michael Kruger and Dr. Stefanie Brachfeld. Dr. Brachfeld, I am forever grateful for you giving me the opportunity to use your amazing Zeiss microscope. Additional thanks to Xiaona Li for helping me run all my samples and trouble-shooting the ICP.

A special thanks to Dr. Thomas Fleming and Dr. Cynthia Coron who more than prepared me for graduate school. Dr. Fleming, it was because of you I grew to love petrology, mineralogy, and instrumentation and without your advising I may have never continued my education. Dr. Coron, your classes were the toughest but they revealed to me just how much I love geology and taught me a whole lot about being self-motivated.

Thank you to everyone in the graduate student office for the entertainment, distractions, and occasionally, help. I will miss you all greatly back in Connecticut, especially during the Game of Thrones season. Catherine and Jessie, I am grateful for your friendship and support these last two years and know that you will always have mine. Jay, what can I say? Without you this thesis would probably have never been completed. Thank you so much for all your help with my field work, ICP preparation, and petrography. But more importantly thank you for your endless support and encouragement.

Last, but far from least, I want to thank my family. Mom and dad, you are the best parents a child could ask for. You always believed in me, even when I doubted myself, and encouraged me to succeed. Dad, thank you for always being willing to talk

science with me and showing an active interest what I love. Mom, you have talked me off the ledge too many times to count; thank you for centering me at my most stressful moments. Don't worry Amy and Sandy, I didn't forget you two. Thank you both for always rooting for me and putting a smile on my face.

TABLE OF CONTENTS

ABSTRACT	i
ACKNOWLEDGEMENTS	iv
LIST OF FIGURES	viii
LIST OF TABLES	ix
1. INTRODUCTION	1
2. REGIONAL GEOLOGIC OVERVIEW	2
3. METHODS	4
3.1. Field Work	4
3.2. Petrographic Methods	4
3.3. Geochemical Methods	5
4. PETROGRAPHY	6
4.1. Thin Section Descriptions	6
4.2. Conclusion	10
5. GEOCHEMISTRY	11
5.1. Major Element Analysis	11
5.2. Trace Element Analysis	14
6. COMPARATIVE GEOCHEMISTRY	15
6.1. Introduction	15
6.2. Geochemical Comparison	16
6.3. Conclusion	19

7. PETROGENESIS	22
7.1. Introduction	22
7.2. Petrogenesis	25
7.3. Conclusion	25
8. CONCLUSION	26
9. REFERENCES CITED	28
APPENDICES	31
Appendix A: Figures	31
Appendix B: Tables	52

LIST OF FIGURES

Figure 1.	Generalized map of the study area	31
Figure 2.	NJ/Hudson Highlands geochronology	32
Figure 3.	Geologic map of the sampling area	33
Figure 4.	Sample locations displayed on topographic map	34
Figure 5.	Select thin section images	35
Figure 6.	REE diagrams	36
Figure 7.	Harker diagram	38
Figure 8.	AFM diagram	43
Figure 9.	FeO/MgO versus TiO ₂ plot	44
Figure 10.	Total alkali-silica plot	45
Figure 11.	Nb, Rb, and Y tectonic discrimination diagrams	46
Figure 12.	Multi-element plots	47
Figure 13.	REE comparisons	49
Figure 14.	Magma generation: mafic samples	50
Figure 15.	Magma generation: intermediate sample w/ HREE depletion	50
Figure 16.	Magma generation: intermediate sample w/ HREE enrichment	51

LIST OF TABLES

Table 1.	Sample locations and descriptions	52
Table 2.	Modal analysis of hypersthene-quartz-oligoclase gneiss	53
Table 3.	ICP-OES reproducibility	54
Table 4.	ICP-MS reproducibility	55
Table 5.	Whole-rock geochemistry	56
Table 6.	List of samples used for comparison	57
Table 7.	Geochemical comparison between units	58
Table 8.	Geochemistry of felsic Losee Suite samples	59
Table 9.	Geochemistry of intermediate Losee Suite samples	60
Table 10.	Geochemistry of mafic Losee Suite samples	61
Table 11.	Geochemistry of felsic metasedimentary rock samples	62
Table 12.	Geochemistry of intermediate metasedimentary rock samples	63
Table 13.	Geochemistry of mafic metasedimentary rock samples	64
Table 14.	Average of specific rock types from the three units	65
Table 15.	Standard deviations of specific rock types from the three units	66
Table 16.	Chondrite and N-MORB normalization values	67

1. INTRODUCTION

Middle Proterozoic rocks of the Hudson and New Jersey Highlands have been the subject of many studies throughout the last century due to their connection to the Grenville orogenic event as well as economic interest in magnetite (Volkert, 2004). During the Grenville orogeny the rock units in these areas were variably deformed and metamorphosed at the upper amphibolite to hornblende-granulite facies conditions, excluding later emplaced pegmatites and coarse-grained granites (Aleinikoff and Grauch, 1990). The rock types associated with this deformational event can be grouped into four general categories: metasedimentary gneisses, metaigneous gneisses, quartzofeldspathic gneisses, and syn-tectonic intrusive granitoid rocks (Dodd, 1965). These rock types constitute the bedrock that underlies the Hudson and New Jersey Highlands, which are part of the greater Reading Prong province. The origin of the gneisses in the Reading Prong has been studied since the mid-1800's and remains controversial for some units. A sedimentary origin was first proposed for the gneisses in the mid-1800's but by the early 1900's a plutonic origin was suggested (Kalczynski, 2012). Not long after, Bayley (1910) proposed that the gneisses represented both plutonic and sedimentary origins, which became the accepted hypothesis. Recently, major element geochemistry has revealed that similarities exist between the major elemental compositions of volcanic rocks and some of the proposed plutonic origin gneisses, specifically the quartzofeldspathic and amphibole-pyroxene gneisses (Kalczynski, 2012). As expected, protolith interpretations of the gneisses can change with time as continued research and advancing analytical techniques yield new data, especially with the addition of trace element analyses. The purpose of this paper is to determine the protolith of the

hypersthene-quartz-oligoclase gneiss from the Hudson Highlands, which is classified as being of unknown origin by Dodd (1965). Gates *et al.* (2001) groups the hypersthene-quartz-oligoclase gneiss with the metavolcanic gneisses in the western Hudson Highlands. Similar units in the New Jersey Highlands are grouped with the Losee Metamorphic Suite by Drake and Volkert (1999) and Volkert (2004). A general lack of available geochemical data for the unit has made protolith determination difficult and in turn prevents it from being definitively grouped with either the metavolcanic or metasedimentary units. This study compares the major element composition of the hypersthene-quartz-oligoclase gneiss samples collected with previously compiled data for the Losee Metamorphic Suite and metasedimentary rocks from Volkert and Drake (1999). Similarities between the major element geochemistry of the hypersthene-quartz-oligoclase gneiss and the Losee Metamorphic Suite would be suggestive of an igneous origin. Conversely, should the geochemistry of the hypersthene-quartz-oligoclase gneiss parallel that of the metasedimentary rocks of the New Jersey Highlands then a sedimentary origin is likely. Rare earth element concentrations within the hypersthene-quartz-oligoclase gneiss will then be used to make hypotheses as to the petrogenesis and tectonic setting that produced this unit.

2. REGIONAL GEOLOGIC OVERVIEW

The Hudson Highlands extend from southern New York until it meets with the contiguous New Jersey Highlands in northern New Jersey. These highlands are part of the greater Reading Prong province, which constitutes one of the largest Grenville-age terrains extending along the northeastern United States (Volkert, 2004). A generalized

map illustrating the spatial relationship between these areas is pictured in Figure 1. The entire Hudson Highlands area is cut into several blocks by northeast- trending high angle faults (Dallmeyer and Dodd, 1971). Metasedimentary, metavolcanic, quartzofeldspathic gneisses, and intrusive granitoid rocks make up the complex assemblage of rocks found throughout the Hudson Highlands region. These dominantly Middle Proterozoic age rock units were variably deformed and metamorphosed at the upper amphibolite to hornblende-granulite facies conditions during the Grenville Orogeny Cycle (1300-1000 Ma), excluding late pegmatites and coarse-grained granite (Aleinikoff and Grauch, 1990). The Grenville orogeny is commonly broken down into a series of orogenic events starting with the Elzevirian orogeny ca. 1300-1200 Ma and ending with the Ottawan orogeny ca. 1100-1000 Ma, see Figure 2 (Volkert, 2004). Similarly, the rocks of the Hudson Highlands can be separated into two basic groups: pre-Ottawan rocks and late to post-Ottawan rocks. Pre-Ottawan rocks, such as the metasedimentary, metavolcanic, and quartzofeldspathic gneisses, have strong, penetrative, high-grade metamorphic fabrics resulting from Ottawan deformation and metamorphism. Conversely, late- to post-Ottawan rocks lack regional scale penetrative fabrics and range from undeformed to locally strong, high-grade, ductile fabrics (Gorring *et al.*, 2003). The hypersthene-quartz-oligoclase gneiss studied in this paper from the Bear Mountain region of New York is currently grouped with gneisses of uncertain derivation by R.T. Dodd (1965) on the geologic map of the Popolopen Lake quadrangle, southeastern New York and with the metavolcanic unit by Gorring *et al.* (2003). Similar units exist in the New Jersey Highlands and are grouped with the Losee Metamorphic Suite by Drake and Volkert (1999) and Volkert (2004)(Figure 2).

3. METHODS

3.1. Field Work

Fifteen samples of the hypersthene-quartz-oligoclase gneiss were collected from the Bear Mountain area of New York (Figures 3 and 4). Sampling locations for this unit were chosen based on the USGS geologic map of the Popolopen Lake Quadrangle (Dodd, 1964) and field observations. The samples that were collected are considered to be representative of the hypersthene-quartz-oligoclase gneiss as they are all mineralogically similar to one another, yet mineralogically distinct from the other gneisses in the area. A summary of sample descriptions and locations can be found in Table 1.

3.2. Petrographic Methods

A thin section was created from each sample and cut from an area that was minimally altered and representative of the bulk rock composition. Rectangular blocks, roughly the size of a thin section, were cut from the hand sample with a diamond-tipped, water lubricated rock saw. The cut blocks were then sent to Spectrum Petrographics Inc. in Vancouver, WA to be made into standard thin sections with no slipcover. Modal analyses were conducted using a Carl Zeiss Axioskop 40 petrographic microscope. Each thin section was divided into six equal quadrants with the modal percentages being noted. The modal analyses from all six quadrants were then averaged to determine the overall modal percentages for that sample. The modal analysis for each sample is summarized in Table 2. Additionally, photographs illustrating typical mineralogy and features of interest were taken using the AxioCam for later reference (Figure 5).

3.3. Geochemical Methods

Sample preparation and analyses were conducted in the laboratories of the Department of Earth and Environmental Studies, Montclair State University, Montclair, New Jersey. Small chips were selected and cut from each sample following the aforementioned petrographic methods. Once approximately 60 g of chips were obtained, they were further broken down using a steel mortar and pestle and dry sieved through a 4.699 mm sieve. The sieved fraction was then powdered in an alumina ceramic shatter box for a period of 5 minutes.

Whole-rock geochemistry of the fifteen hypersthene-quartz-oligoclase gneiss samples was determined using the Jobin-Yvon inductively-coupled plasma optical emission spectrometer (ICP-OES) for major element analysis and the Thermo-Electron inductively coupled plasma mass spectrometer (ICP-MS) for trace element analysis. Powder from each sample weighing 0.1000 g (\pm 0.0005 g) was added to 0.4000 g (\pm 0.0020 g) of lithium metaborate flux and manually homogenized. The mixtures were then transferred to graphite crucibles, which were placed in a furnace for fusion at 1,050°C for approximately 20 minutes. After the 20 minute fusion period, the molten samples were poured into 50 mL of 7% nitric acid to produce master solutions with a dilution factor of 500X. Dissolution was aided by magnetic stir bars until solid sample was no longer visible in the solution. All solutions were filtered to remove any residual graphite remaining from the crucibles. Master solutions were also made for two blanks and ten USGS rock standards, DNC-1, BIR-1, BHVO-2, W-2, BCR-2, AGV-2, QLO-1, GSP-2, G-2, and RGM-1.

Solutions for major element analysis using the ICP-OES were created by combining 6.5 mL of master solution from each sample with 50 mL of 2% nitric acid, resulting in a solution with a dilution factor of 4,000X. Similarly, solutions for trace element analysis using the ICP-MS were created by combining 2.5 mL of master solution from each sample with 50 mL of 2% nitric acid, resulting in a solution with a dilution factor of 10,000X. Major and trace element data reported in this paper are the result of an average of four replicate runs. A drift solution was measured after every fourth sample to correct for variations in the instrument's sensitivity.

Analytical precision and accuracy of the ICP-OES and ICP-MS was determined by measuring eight replicates of one hypersthene-quartz-oligoclase gneiss sample (BM-11) and one USGS rock standard (AGV-2). The results, which are reported in Tables 3 and 4, are the average of three replicate runs. Instrument precision for the ICP-OES is \pm 0.5-3.4%, except for MnO (\pm 3.0-6.9%). The accuracy for the ICP-OES based on USGS standard AGV-2 values is \pm 1.1-2.3%, except for MnO, which is \pm 8.0%. Instrument precision for the ICP-MS is generally \pm 1-10% with Sc, Cr, Y, Cs, Pb, and Th being exceptions. The accuracy for the ICP-MS based on USGS standard AGV-2 values is \pm 0.1-10.3%, except for Ni, Y, Cs, La, and Pb.

4. PETROGRAPHY

4.1. Thin Section Descriptions

Some petrographic features are common to all of the hypersthene-quartz-oligoclase gneiss samples summarized here and will not be mentioned in further descriptions unless variations were noted. Samples are typically hypidioblastic with

subhedral to anhedral feldspars, anhedral quartz, subhedral to euhedral biotite, and subhedral to anhedral pyroxenes. Polysynthetic (albite) twinning is typical of the plagioclase feldspar while tartan twinning is typical of the potash feldspar. Alteration in the samples is usually in the form of sericite and occasionally chlorite.

BM-1: Sample is medium grained with the dominant mineralogy being 60% plagioclase feldspar, 20% quartz, 8% biotite, 7% orthopyroxene, 3% clinopyroxene, and 2% alteration. Trace amounts of opaques are present. Both orthopyroxene and clinopyroxene are mildly to moderately altered and exhibit typical pale pink to pale green pleochroism. Clinopyroxene displays middle second order interference colors while orthopyroxene is commonly middle first order pale grey.

BM-2: Sample is medium grained with the dominant mineralogy being 68% plagioclase feldspar, 14% quartz, 6% biotite, 5% orthopyroxene, 3% clinopyroxene, 3% alteration, and 1% opaques. Clinopyroxene displays middle second order interference colors while orthopyroxene is commonly lower first order pale yellow.

BM-3: Sample is medium grained with the dominant mineralogy being 53% plagioclase feldspar, 36% quartz, 6% biotite, 3% orthopyroxene, 1% potash feldspar, and 1% alteration. Trace amounts of opaques and zircon are present. Plagioclase was largely unaltered although wart-like and rim myrmekite were visible within some grains. Potash feldspar appears sporadically throughout the sample as small anhedral grains. Minute zircon crystals are euhedral to subhedral.

BM-4: Sample is medium grained with the dominant mineralogy being 54% plagioclase feldspar, 39% quartz, 4% biotite, 1% orthopyroxene, and 2% alteration. Trace amounts of opaques and zircon are present. Orthopyroxene is only mildly altered.

BM-5: Sample is fine grained with the dominant mineralogy being 66% plagioclase feldspar, 21% quartz, 9% biotite, 2% garnet, and 2% alteration. Trace amounts of opaques and zircon are present. Garnet is poikiloblastic, subhedral, and present as large grains. Although zircon is only present in trace amounts, it is more prevalent in this sample than the rest of the unit.

BM-6: Sample is fine grained with the dominant mineralogy being 56% quartz, 45% potash feldspar, 24% biotite, and 5% plagioclase feldspar. Trace amounts of opaques and zircon are present. The sample overall shows little to no alteration.

BM-7: Sample is fine grained with the dominant mineralogy being 43% plagioclase feldspar, 29% potash feldspar, 22% quartz, 4% biotite, and 2% alteration. Rim myrmekite was occasionally spotted surrounding portions of plagioclase feldspar grains.

BM-8-T: Sample is medium grained with the dominant mineralogy being 48% plagioclase feldspar, 17% potash feldspar, 15% biotite, 8% clinopyroxene, 7% orthopyroxene, and 5% quartz. Trace amounts of alteration is present. Clinopyroxene displays middle second order blue-green interference colors while orthopyroxene is commonly lower first order pale grey. Many of the clinopyroxene have exsolution lamellae.

BM-8-M: Sample is fine grained with the dominant mineralogy being 30% plagioclase feldspar, 44% potash feldspar, 17% quartz, 4% orthopyroxene, 2% biotite, 2% opaques, and 1% alteration. Orthopyroxene displays middle first order yellow interference color and is often moderately altered.

BM-8-B: Sample is medium grained with the dominant mineralogy being 49% plagioclase feldspar, 20% potash feldspar, 12% biotite, 7% quartz, 5% orthopyroxene,

3% opaques, 2% alteration, 1% clinopyroxene, and 1% hornblende. Trace amounts of zircon is present. Opaques are commonly in the form of thin lathes and found in association with biotite. Clinopyroxene displays low second order pink interference colors while orthopyroxene is commonly lower first order pale grey. Hornblende appears as subhedral crystals and distinguished from the pyroxenes and biotite by its pleochroism and cleavage.

BM-9: Sample is medium grained with the dominant mineralogy being 47% plagioclase feldspar, 3% potash feldspar, 12% hornblende, 12% quartz, 10% biotite, 7% clinopyroxene, 5% orthopyroxene, 3% alteration, and 1% opaques. Both clinopyroxene and orthopyroxene have exsolution lamellae with it being more common in the former. Hornblende appears as large subhedral to anhedral crystals.

BM-10: Sample is medium grained with the dominant mineralogy being 69% plagioclase feldspar, 9% biotite, 8% hornblende, 7% alteration, 4% quartz, 2% garnet, and 1% opaques. Hornblende is subhedral to anhedral. Garnet appears as large, anhedral crystals.

BM-11: Sample is medium grained with the dominant mineralogy being 68% plagioclase feldspar, 24% quartz, 3% biotite, 3% orthopyroxene, and 2% potash feldspar. The sample also contains trace amounts of opaques and zircon.

BM-12: Sample is medium grained with the dominant mineralogy being 59% plagioclase feldspar, 35% quartz, 3% biotite, 2% potash feldspar, and 1% alteration.

BM-13: Sample is fine grained with the dominant mineralogy being 52% potash feldspar, 41% quartz, 3% plagioclase feldspar, 2% biotite, and 2% alteration. Trace

amounts of opaques and zircon are also present. Wartlike myrmekite occurs sporadically throughout sample.

4.2. Conclusion

Modal analyses of the thin sections are presented in Table 2. The modal ranges of the felsic minerals within the hypersthene-quartz-oligoclase gneiss samples collected are as follows: 30-69% plagioclase feldspar, 0-44% potassic feldspar, and 4-39% quartz. Mafic mineral modal ranges in the hypersthene-quartz-oligoclase gneiss are: 0-12% hornblende, 2-15% biotite, 0-8% clinopyroxene, 0-7% orthopyroxene, 0-2% garnet, and 0-3% opaque minerals. Additionally, there is zero to trace amounts of zircon and 0-7% alteration products. Note that modal ranges do not include percentages from samples BM-6 and BM-13. Modal analysis of samples BM-6 and BM-13 revealed a distinct difference in their mineralogy that leads one to believe they are not considered representative of the hypersthene-quartz-oligoclase gneiss as a unit. Their high percentages of potassic feldspar and quartz accompanied by exceptionally low plagioclase feldspar are uncharacteristic of the suite of samples. The disparity between BM-6 and BM-13 and the rest of the samples collected is further supported by the weight percent of SiO₂, MgO, and K₂O reported in the whole-rock geochemistry (Table 5) and the patterns they produce on a REE plot (Figure 6). These samples could possibly be the result of potassium feldspar rich lenses within the hypersthene-quartz-oligoclase unit or could interlayers of associated quartz-plagioclase leucogneiss, which generally contains greater amounts of potassic feldspar than the hypersthene-quartz-oligoclase gneiss. Due to the considerable mineralogic and geochemical difference between these two samples and the rest of the unit they will not be utilized in further portions of this study for

protolith determination. However, they are still included in ensuing geochemical plots but are easily recognized due to their high silica contents (75.8% and 73.1%).

The mineralogy of the hypersthene-quartz-oligoclase gneiss when compared to that of the Losee Metamorphic Suite and metasedimentary rocks of the New Jersey Highlands more closely resembles that of the former. Typically, the hypersthene-quartz-oligoclase gneiss lacks the minerals garnet, sillmanite, and graphite, which occur throughout many of the metasedimentary rocks. Additionally, some of the metasedimentary rocks contain clinopyroxene but orthopyroxene is absent from all. Conversely, orthopyroxene is often present in greater than 5% in the charnockitic rocks of the Losee Metamorphic Suite (Volkert and Drake, 1999).

5. GEOCHEMISTRY

5.1. Major Element Analysis

Major element analysis of the hypersthene-quartz-oligoclase gneiss samples was conducted using the ICP-OES. The findings are summarized in Table 5. General major element observations can be made for the suite of samples based on their abundances of these elements and trends displayed on variation diagrams of weight % oxides versus weight % SiO₂ (Figure 7). The following discussion summarizes the compositional variations within the suite of samples on an element-by-element basis.

Weight % SiO₂ varies within the suite of samples, ranging from silica-undersaturated at 48.4% up to silica-oversaturated at 75.8%. Due to this variability it proves useful to group the samples according to their SiO₂ content. Samples containing 70% SiO₂ or greater were considered felsic, between 55-70% SiO₂ intermediate, and 55%

or less SiO_2 were regarded as mafic. A list of the samples within each compositional group is given in Table 6. Of the fifteen samples collected two are felsic, nine are of intermediate composition, and four are mafic.

The overall weight % of TiO_2 ranges from 0.1% to 1.9% through the entire suite of samples. TiO_2 ranges from 0.1% to 0.6% in felsic samples, 0.4% to 1.0% in intermediate samples, and 1.5% to 1.9% in mafic samples. Generally, TiO_2 decreases with increasing SiO_2 .

Al_2O_3 ranges from 11.9% to 21.4% throughout the suite of samples. In general, Al_2O_3 decreases with increasing SiO_2 although this trend is not apparent in the spread of strictly the mafic samples, which have a wide range of Al_2O_3 values. Weight % Al_2O_3 ranges from 11.9% to 15.1% in felsic samples, 16.1% to 19.5% in intermediate samples, and 14.6% to 21.4% in mafic samples.

Weight % Fe_2O_3 in the suite of samples ranges from 0.4% to 13.1%. Fe_2O_3 ranges from 0.4% to 2.3% in felsic samples, 2.8% to 7.5% in intermediate samples, and 10.3% to 13.1% in mafic samples. On a variation diagram, weight % Fe_2O_3 shows a marked decrease with increasing SiO_2 .

MnO values are commonly less than 0.1% with a few exceptions. In felsic samples, MnO ranges from below detection limit up to 0.01%. MnO values range from 0.01% to 0.1% in intermediate samples and from 0.05% to 0.1% in mafic samples. Generally, MnO decreases with increasing SiO_2 . However, there is a wide spread in the MnO values for the intermediate samples, which is also seen to a lesser extent within the mafic samples.

MgO ranges from 0.3% to 6.4% through the suite of samples. MgO values range from 0.3% to 1.2% in felsic samples, 1.2% to 3.8% in intermediate samples, and 2.6% to 6.4% in mafic samples. On a variation diagram, weight % MgO decreases with increasing SiO₂.

The weight % of CaO ranges from 1.0% to 8.6% throughout the suite of samples. CaO values are about 1.0% in felsic samples, range from 2.9% to 7.0% in intermediate samples, and 4.6% to 8.6% in mafic samples. Generally, weight % CaO decreases with increasing SiO₂. The low CaO values observed in samples BM-6, BM-8-M, and BM-13 coincide with the mineralogy of those samples, mainly that they have lower modal percentages of plagioclase feldspar than other samples within the suite.

Na₂O ranges from 2.5% to 4.7% throughout the suite of samples. Weight % Na₂O is about 2.9% in the felsic samples, ranges from 3.1% to 4.7% in the intermediate samples, and 2.5% to 4.2% in the mafic samples. When plotted against weight % SiO₂, no correlation could be made between Na₂O and increasing SiO₂.

K₂O ranges from 1.4% to 6.5% within the suite of samples. The weight % of K₂O ranges from 3.2% to 6.5% in the felsic samples, 1.4% to 4.2% in the intermediate samples, and 2.7% to 3.6% in the mafic samples. The variations in K₂O in these samples do not correlate with increasing SiO₂.

Weight % P₂O₅ ranges from 0.1% up to 0.6% through the suite of samples. P₂O₅ is about 0.1% in the felsic samples, ranges from 0.2% to 0.30% in the intermediate samples, and 0.2% to 0.6% in the mafic samples. Generally, P₂O₅ decreases with increasing SiO₂.

Based on the preceding observations, a few general trends of the major elements in the hypersthene-quartz-oligoclase gneiss samples collected can be summarized. First, the samples can be grouped by their varied SiO_2 content into felsic, intermediate, and mafic rocks. Secondly, TiO_2 , Al_2O_3 , Fe_2O_3 , MnO , MgO , CaO , and P_2O_5 all decrease with increasing SiO_2 . Lastly, no correlation could be made between the alkalis, Na_2O_3 and K_2O , and increasing SiO_2 .

5.2. Trace Element Analysis

Trace element analysis of the hypersthene-quartz-oligoclase gneiss samples collected was conducted using the ICP-MS. The following discussion focuses on summarizing the abundances and general trends of trace elements that fall into specific element groups, mainly large ion lithophile elements (LILE), high field strength elements (HFSE), rare earth elements (REE). Table 5 contains a complete list of the trace elements analyzed and their abundances within each sample.

Trace elements analyzed that are LILE include Rb, Sr, Cs, and Ba. The concentrations of these elements within the suite of samples are as follows: Rb 51-367 ppm, Sr 108-502 ppm, Cs 0.5-6.1 ppm, and Ba 143-1291 ppm. The highest concentrations of these elements are found in the BM-8 samples. However, the highest concentration measured of Sr is in BM-4. High field strength trace elements that were measured include Zr, Hf, Nb, and Ta. The concentrations of these elements within the suite of samples are as follows: Zr 47-586 ppm, Hf 1-13 ppm, Nb 3-37 ppm, and Ta 0.13-1.95 ppm. The highest concentrations of these elements are found in the BM-8 samples, excluding U, which is highest in BM-6. In terms of REE characteristics, all samples are light rare earth element (LREE) enriched in comparison to the heavy rare earth elements

(HREE) with the exception of BM-6. BM-8-M and BM-8-B have the highest enrichment of LREEs. Samples that are HREE enriched include BM-1, BM-2, BM-5, BM-6, BM-8-T, BM-8-M, BM-8-B, BM-9, and BM-10. Samples that are depleted in HREE include BM-3, BM-4, BM-7, BM-11, BM-12, and BM-13 with BM-4 and BM-7 being the most depleted. Figure 6 illustrates the REE abundance patterns described above.

6. COMPARATIVE GEOCHEMISTRY

6.1. Introduction

Mineralogically and geochemically similar units to the hypersthene-quartz-oligoclase gneiss from the Hudson Highlands occur throughout the physically contiguous New Jersey Highlands (Drake and Volkert, 1995). As such, a geochemical comparison between the hypersthene-quartz-oligoclase gneiss and the units in New Jersey could prove useful when attempting protolith determination of the former. Geochemical similarities between the hypersthene-quartz-oligoclase gneiss and the Losee Metamorphic Suite would be suggestive of an igneous origin. Conversely, should the geochemistry of the hypersthene-quartz-oligoclase gneiss parallel that of the metasedimentary rocks of the New Jersey Highlands then a sedimentary origin should be investigated. The following sections summarize geochemical characteristics that are shared between the hypersthene-quartz-oligoclase gneiss, Losee Metamorphic Suite, and the metasedimentary unit.

Due to the wide range of SiO₂ content in the suite of samples collected for this study, comparisons between units included only samples within specific SiO₂ ranges so as to prevent skewing of the data. Samples are grouped as follows: >70% SiO₂ is felsic, 55-70% SiO₂ is intermediate, and < 55% SiO₂ is mafic. The averaged geochemical data

from all samples within each SiO₂ group were averaged to facilitate comparisons between units (Table 7). Only samples that are mineralogically, texturally, and geochemically similar to the hypersthene-quartz-oligoclase gneiss are chosen from the New Jersey Highlands samples. Table 6 contains a full list of the hypersthene-quartz-oligoclase gneiss, Losee Metamorphic Suite, and metasedimentary unit samples compared within each SiO₂ group. All data pertaining to the Losee Metamorphic Suite and metasedimentary rocks is taken from Drake and Volkert (1999). The following major element oxides (weight %) and trace elements (ppm) are the basis of comparison: TiO₂, Al₂O₃, FeO_{Total}, MnO, MgO, CaO, Na₂O₃, K₂O, P₂O₅, Ba, and Sr. These oxides were selected based on the availability of geochemical data for the Losee Metamorphic Suite and the metasedimentary rocks of the New Jersey Highlands.

6.2. Geochemical Comparison

Losee Metamorphic Suite samples used for geochemical comparison with the hypersthene-quartz-oligoclase gneiss include the following rock units: (Ylo) quartz-oligoclase gneiss, (Ylb) biotite-quartz-oligoclase gneiss, (Yh) layered charnockitic rocks, and (Yd) massive charnockitic rocks. The metasedimentary rock samples used for geochemical comparison include the following units: (Yb) biotite-quartz-feldspar gneiss, (Ymh) hornblende-quartz-feldspar gneiss, (Ymp) clinopyroxene-quartz-feldspar gneiss, and (Yp) pyroxene gneiss. Metasedimentary rock samples from the aforementioned units containing appreciable amounts of serpentine and epidote were not used for comparison as the mineralogy is not consistent with that of the hypersthene-quartz-oligoclase gneiss. All rock unit names and abbreviations are reported as they were mapped by Drake *et al.* (1996). The discussion of the geochemical comparisons between the three units will be

divided up according to the oxides and trace elements investigated. Table 7 summarizes the averaged geochemical data that is the basis of comparison.

TiO₂: No appreciable difference in TiO₂ is noted between the three units within the felsic and intermediate categories. However, in the mafic samples TiO₂ in hypersthene-quartz-oligoclase gneiss is nearly twice that of the Losee Metamorphic Suite and the metasedimentary rocks.

Al₂O₃: Within the felsic samples there is little variation between the units with Al₂O₃ being ~13.0% for all three. The percent Al₂O₃ in intermediate and mafic hypersthene-quartz-oligoclase gneiss samples is notably closer to that of the Losee Metamorphic Suite than that of the metasedimentary rocks.

FeO_{Total}: FeO_{Total} for the hypersthene-quartz-oligoclase gneiss is marginally closer to the Losee Metamorphic Suite in both felsic and mafic samples. Little variation is present between intermediate samples of the three units which are all between ~4.3-4.8% FeO_{Total}.

MnO: All three units have only minor amounts of MnO at less than 0.2%. Generally, MnO is highest in metasedimentary rocks and lowest in the hypersthene-quartz-oligoclase gneiss.

MgO: Within the felsic and intermediate sample, MgO is greatest in the hypersthene-quartz-oligoclase gneiss and slightly closer to the Losee Metamorphic Suite values. Conversely, in the mafic samples hypersthene-quartz-oligoclase gneiss MgO at 4.5% is comparable to the metasedimentary rocks (4.4%) rather than the Losee Metamorphic Suite (6.5%).

CaO: CaO for the hypersthene-quartz-oligoclase gneiss is similar to that of the metasedimentary rocks in the felsic samples with both being ~1.0%. Within the samples of intermediate composition, hypersthene-quartz-oligoclase gneiss at 4.4% is higher than the other two units but slightly closer to the Losee Metamorphic Suite (3.8%). CaO is considerably lower in hypersthene-quartz-oligoclase gneiss (7.5%) than both the Losee Metamorphic Suite (11.2%) and metasedimentary rocks (14.6%).

Na₂O: Felsic samples from all three units have variable Na₂O with the Losee Metamorphic Suite having the highest at 5.0%, then the metasedimentary rocks at 3.8%, and hypersthene-quartz-oligoclase gneiss having the least at 2.9%. Within the intermediate samples, Losee Metamorphic Suite and the metasedimentary rocks contain ~5.0% Na₂O while the hypersthene-quartz-oligoclase gneiss contains ~4.0%. Na₂O values for mafic samples of the hypersthene-quartz-oligoclase gneiss are more closely related to that of the metasedimentary unit.

K₂O: K₂O values in the felsic samples are comparable for the metasedimentary samples and hypersthene-quartz-oligoclase gneiss being close to 5.00% versus the Losee Metamorphic Suite which is ~2.0%. Within the intermediate samples, the Losee Metamorphic Suite and hypersthene-quartz-oligoclase gneiss contain about 2.0% K₂O while the metasedimentary rocks have ~3.0%. Notably, K₂O in the mafic samples is much higher in hypersthene-quartz-oligoclase gneiss at 3.1% than the other two units, which have less than 1.0%.

P₂O₅: The average percent of P₂O₅ throughout all samples compositions is less than 0.5%. P₂O₅ in the felsic samples of the metasedimentary rocks is nearly twice that of felsic Losee Metamorphic Suite and hypersthene-quartz-oligoclase gneiss samples. P₂O₅

in intermediate composition samples is ~0.2% in all three units. Within the mafic samples, P_2O_5 was close to 0.4% in the hypersthene-quartz-oligoclase gneiss and metasedimentary rocks which is nearly three times that of the Losee Metamorphic Suite samples.

Ba and Sr: Generally, in felsic and intermediate samples, the Ba/Sr ratios are similar between the Losee Metamorphic Suite and hypersthene-quartz-oligoclase gneiss. In the metasedimentary rocks, Ba is about 5.5x that of Sr in felsic samples and about 3x Sr in intermediate samples. Within the mafic samples there is no apparent connection between the three units.

6.3. Conclusion

Characterizing broad geochemical trends within each unit, as well as similarities shared between units, proves to be a difficult task as the geochemistry varies greatly over the wide range of silica contents. Generally, there are few appreciable geochemical differences between the major element averages for the samples chosen for comparison summarized in Table 7. Further illustration of the similarities in the major element geochemistry between the selected samples of these three units is provided by Figures 8-10. The fact that the compositions of the metasedimentary rocks and Losee Metamorphic Suite fall into similar fields when plotted on all three diagrams attests to the similar geochemistry between the two. One possible explanation for the overlap in geochemistry between the two units be that the origin of the sediment that produced the metasedimentary protolith was eroded from the Losee Suite which is believed to be older based on the stratigraphy of the area. However, these apparent similarities could also be the effect of two things: sample selection and averaging. Samples from the Losee Suite

and metasedimentary rocks were chosen on the basis of comparable mineralogy and silica content to the hypersthene-quartz-oligoclase gneiss. Therefore, they are similar to the unit of interest but may not be completely representative of their unit. This selection method in turn leads to problems when it comes to interpreting the averaged data from Table 7. Perhaps the most prominent relationship displayed in Table 7 between the three units involves their respective average Al_2O_3 content. Although, the average Al_2O_3 is consistent between the Losee Metamorphic Suite and metasedimentary rocks in the felsic samples, it becomes notably higher in the Losee rocks when compared to the metasedimentary rocks in the intermediate and mafic compositional groups. The Al_2O_3 content within the hypersthene-quartz-oligoclase gneiss is comparable to that of the Losee Metamorphic Suite rather than the metasedimentary rocks. The typical range in Al_2O_3 for the Losee Metamorphic Suite is between 12-19% as reported by Volkert and Drake (1999) which compares well to the ~14-21% of the hypersthene-quartz-oligoclase gneiss (Table 5).

In order to counteract some of the negative effects of averaging the data, Tables 8-13 were generated for additional geochemical comparison. One variation between the Losee Suite and the metasedimentary rocks chosen is that CaO is typically greater in the Losee rocks than the metasedimentary rocks. Within the felsic compositional group, the Losee Metamorphic Suite samples selected have an average CaO value of 2.4% with a standard deviation of 0.8 while the metasedimentary rocks have 1.2% CaO with a standard deviation of 0.6. This trend continues with samples of intermediate composition with the exception the pyroxene gneiss samples from the metasedimentary unit, which have unusually high percentages of CaO (an average of 5.2%). The intermediate

composition Losee Suite samples selected had an average CaO of 3.8% with a standard deviation of 1.1 while those of Yb and Ymp from the metasedimentary unit contain less than 2.0%. CaO content of the intermediate samples of hypersthene-quartz-oligoclase gneiss ranges from roughly 3-7% with an average of 4.4%, which is comparable to the Losee Metamorphic Suite values. In addition to the difference in CaO between the metasedimentary unit and that of the Losee Metamorphic Suite and hypersthene-quartz-oligoclase gneiss there is notable trend in the ratios of Na₂O to K₂O. As is common for rocks of volcanic origin, the Losee Suite rocks have more Na₂O compared to K₂O (Winter, 2010). The average Na₂O/K₂O ratio of the felsic Losee samples chosen is 2.6 and 3.0 in the intermediate samples. Conversely, rocks of sedimentary origin usually have a higher percentage of K₂O compared to Na₂O leading to lower Na₂O/K₂O ratios (Winter, 2010). Metasedimentary rocks within the felsic compositional group display a typical low Na₂O/K₂O ratio of 0.8 and remain low for most of the units in the intermediate compositional group (Yb: 1.3 and Ymh: 0.7) except for the pyroxene gneiss (8.6). Generally, the hypersthene-quartz-oligoclase gneiss has slightly higher Na₂O/K₂O ratios than the average rock within the metasedimentary unit. Tables 14 and 15 summarize the averages and standard deviations of the specific rock types chosen from the Losee Metamorphic Suite, metasedimentary rocks, and the hypersthene-quartz-oligoclase gneiss. To summarize, the high Al₂O₃ and CaO percentage coupled with a moderate Na₂O/K₂O ratio is comparable to that of the metavolcanic Losee Metamorphic Suite rather than the metasedimentary rocks.

7. PETROGENESIS

7.1. Introduction

General classification of the hypersthene-quartz-oligoclase gneiss as either igneous or sedimentary origin is based on the similarities that exist between the unit and that of the Losee Metamorphic Suite or metasedimentary rocks of the New Jersey Highlands. Previously stated similarities have been shown to exist between the hypersthene-quartz-oligoclase gneiss and the Losee Suite, which will be summarized here. Mineralogically, the two units both contain orthopyroxene, which is absent from the metasedimentary rocks. Additionally, the metasedimentary rocks contain a greater modal percent of potassic feldspar than the Losee Suite and hypersthene-quartz-oligoclase gneiss. Geochemically, Losee Metamorphic Suite rocks and hypersthene-quartz-oligoclase gneiss have an appreciably higher average Al_2O_3 content compared to the metasedimentary rocks. Generally, the Losee Suite rocks and hypersthene-quartz-oligoclase gneiss also have higher CaO values and $\text{Na}_2\text{O}/\text{K}_2\text{O}$ ratios than the metasedimentary rocks. Based on these observations, the protolith of the hypersthene-quartz-oligoclase gneiss is likely similar to that of the Losee Metamorphic Suite. As such, the ensuing petrogenetic discussion will focus on investigating an igneous origin for the unit.

7.2. Petrogenesis

The major element geochemistry for the hypersthene-quartz-oligoclase gneiss is presented in Table 5 and further illustrated on the Harker diagrams in Figure 7. On a total alkali versus silica plot, the hypersthene-quartz-oligoclase gneiss composition ranges from basalt to dacite (Figure 10). The majority of hypersthene-quartz-oligoclase

gneiss samples plot within the calc-alkaline field on an AFM diagram (Figure 8). Calc-alkaline series magma is typical of convergent plate margin tectonic settings and often produces calc-alkaline volcanic rocks of andesitic, dacitic, and less commonly rhyolitic compositions (Harangi *et al.*, 2007). On a diagram of FeO/MgO versus TiO₂, most of the hypersthene-quartz-oligoclase gneiss samples plot within the continental arc margin range (Figure 9). Additional support for an arc margin tectonic setting origin for this unit comes from trace element data. Tectonic discriminant diagrams in Figure 11 show that generally the hypersthene-quartz-oligoclase gneiss plots within the volcanic arc granite field. An arc margin tectonic setting for these rocks is to be expected as age relations relate them to the Elzevirian Orogeny (Gates *et al.*, 2001).

Rare earth element (REE) data for the hypersthene-quartz-oligoclase gneiss is summarized in Table 5 and plotted on REE diagrams (Figure 4) and multi-element diagrams (Figure 12). Analysis of REE element trends allows for a more detailed petrogenetic analysis. Trace element compositions of the samples are grouped according to similar silica compositions and HREE depletion/enrichment patterns on the REE and multi-element diagrams. One reason for this grouping is to mitigate crowding of the REE patterns. The other reason for this grouping is to allow for better visualization of the wide range in REE patterns plotted. The multi-element diagrams in Figure 12 generally show LILE enrichment in respect to the elements Rb, Ba, and K and depletion in HFS elements Nb, Ta, Hf, and Ti which is characteristic of subduction zone magmas produced by fluid flux melting of the mantle material due to dewatering of the subducting oceanic crust and sediments (Winter, 2010). LILE enrichment occurs in subduction zone settings due to the fluid mobilization of those elements derived from the subducted sediments

(Sorenson *et al.*, 1997). Depletion of HFSEs in subduction settings could be the result of a number of processes which are still debated. One proposed mechanism for HFSE depletion in arc magmas is that the mantle source has undergone extensive previous melt extractions leading to depletion of those elements in that portion of the mantle. Another plausible explanation involves the stabilization of minerals such as rutile or ilmenite due to fluids derived from the subducting slab and sediments which incorporate HFSEs into their crystalline structure (Arculus, 1987). However, some of the samples do show depletion in Th and U but depletion of these elements has been known to occur in granulite facies terrains (Rudnick and Presper, 1990).

REE patterns of the hypersthene-quartz-oligoclase gneiss are not indicative of crystal fractionation from a single parent magma. All samples are LREE enriched in comparison the HREE. However, the concentrations of HREE range in intermediate composition samples from depleted to moderately enriched, with many of the samples being more depleted than the mafic composition samples. The mafic samples of the hypersthene-quartz-oligoclase gneiss are considered to be representative of the primitive parent magma that would have produced the intermediate samples and were thus used as the basis of comparison. A parent-daughter relationship for crystal fractionation cannot be made based on the samples collected as many of the potential daughters of intermediate composition are HREE depleted compared to mafic compositions that could represent parent magma (Figure 13). Additionally, a parent-daughter relationship cannot be inferred from the REE patterns of the mafic composition samples and the intermediate composition samples that are relatively enriched in HREE because the slope between the two is not preserved added to the fact that the Eu anomalies are not consistent (Winter,

2010)(Figure 13). The lack of an apparent parent-daughter relationship between samples could be the result of insufficient sampling. However, in the case of the HREE depleted intermediate composition samples this would require a parent mafic magma with an even more HREE depletion.

7.3. Conclusions

The major and trace element geochemistry of the hypersthene-quartz-oligoclase gneiss is predominantly of calc-alkaline affinity ranging in composition from basalt to dacite. Calc-alkaline rocks are typical of convergent margin, subduction zone tectonic settings. The overall LREE and LILE enrichment coupled with HFSE depletion of the suite further supports this tectonic setting. The mafic composition samples are interpreted to be produced by fluid-flux partial melting of spinel lherzolite in the asthenospheric mantle wedge due to dehydration of the subducting oceanic crust and sediments (Winter, 2010) (Figure 14). Data from REE plots generally do not indicate that the intermediate hypersthene-quartz-oligoclase gneiss samples were produced by crystal fractionation from a single mafic parent magma. Some of the intermediate samples with moderate HREE enrichment could be the result of crystal fractionation from a mafic magma relatively enriched in HREE's similar to those collected for this study, but with lower REE concentrations. An alternative hypothesis for the petrogenesis of the intermediate samples is they are the product of direct partial melts of the mafic lower continental arc crust (e.g. underplated arc basalts). The intermediate composition samples with HREE depletion are likely generated from direct partial melting of the mafic lower crust in a thickened continental crust where garnet is stable (e.g. partial melting of garnet amphibolite) (Figure 15). The intermediate composition samples with

HREE enrichment are likely generated from partial melting of the mafic lower crust at shallower depths where garnet is not present (e.g. partial melting of garnet-free amphibolite) (Figure 16).

8. CONCLUSION

Mineralogically and geochemically, the hypersthene-quartz-oligoclase gneiss from the Hudson Highlands more closely resembles the Losee Metamorphic Suite than the metasedimentary rocks. Typically, the metasedimentary rocks contain sillimanite, garnet, and/or graphite and lack orthopyroxene. Rock units within the Losee Metamorphic Suite and the hypersthene-quartz-oligoclase gneiss contain orthopyroxene, with sillimanite being completely absent, and garnet and graphite occasionally present as trace components. The similarities between the Losee Suite and hypersthene-quartz-oligoclase gneiss are further paralleled in their major element geochemistry. Generally, both units have higher Al_2O_3 , CaO, and $\text{Na}_2\text{O}/\text{K}_2\text{O}$ ratios than the metasedimentary rocks (Volkert and Drake, 1999). Based on the mineralogic and geochemical similarities present between the hypersthene-quartz-oligoclase gneiss and the Losee Metamorphic Suite the protolith of the former was likely of igneous origin rather than sedimentary.

The bulk-rock geochemistry of the hypersthene-quartz-oligoclase gneiss is of calc-alkaline affinity, which is typical of convergent margin, subduction zone tectonic settings. The overall LILE enrichment, HFSE depletion, and LREE enrichment compared to the HREE's is indicative of a magma generated from sources that were produced by fluid-flux melting due to dehydration of the subducting oceanic crust and sediments. REE plots of the samples point to multiple sources of magma, which

produced the protolith of the hypersthene-quartz-oligoclase gneiss. Intermediate composition samples with moderate HREE enrichment could be the result of crystal fractionation from a mafic parent; magma relatively enriched in HREE's or the product of direct partial melts of the mafic lower continental crust in the absence of garnet. Intermediate composition samples with strong HREE depletion represent magmas produced by direct partial melting of garnet amphibolite in a thickened lower continental crust. Mafic composition samples have typical calc-alkaline arc signatures produced by the partial melting of spinel lherzolite in the asthenospheric mantle wedge caused by dehydration of the subducting oceanic crust and sediments (Winter, 2010).

9. REFERENCES CITED

- Aleinikoff, J. N., and Grauch, R.I., 1990, U-Pb geochronologic constraints on the origin of a unique monazite-xenotime gneiss, Hudson Highlands, New York: American Journal of Science, v. 290, p. 255-546.
- Arculus, R.J., 1987, The significance of source versus process in the tectonic controls of magma genesis: Journal of Volcanology and Geothermal Research, v. 32, p. 1-12.
- Bayley, W.S., 1910, Iron mines and mining in New Jersey: New Jersey Geological Survey, Final Report, v. 7.
- Dallmeyer, R. D., and Dodd, R.T., 1971, Distribution and significance of cordierite in paragneisses of the Hudson Highlands, Southern New York: Contributions to Mineralogy and Petrology, 33, p. 289-308.
- Dodd, R.T., 1965, Precambrian geology of the Popolopen Lake quadrangle, Southeastern New York: New York State Museum and Science Service, Geologic Map and Chart Series Number 6.
- Drake, A.A., Jr., Volkert, R.A., Monteverde, D.H., Herman, G.C., Houghton, H.F., Parker, R.A., and Dalton, R.F., 1996, Bedrock geologic map of New Jersey: U.S. Geologic Survey Miscellaneous Investigations Series Map I-2540-A, 2 sheets, scale 1:100,000.
- Drake, A.A., Jr., and Volkert, R.A., 1999, Geochemistry and stratigraphic relations of Middle Proterozoic rocks of the New Jersey Highlands: U.S. Geological Survey Professional Paper 1565-C.
- Gates A.E., Valentino, D.W., Goring, M.L., Chiarenzelli, J.R., and Hamilton, M.A., 2001, Bedrock geology, geochemistry, and geochronology of the Grenville

- Province in the western Hudson Highlands, New York: In Gates, A.E., ed., 73rd New York State Geological Association Guidebook, p. 176-203.
- Gorring, M.L., Valentino, D.W., Solar, G.S., and Gates, A.E., 2003, Late Ottawaan ductile shearing and granitoid emplacement in the Hudson Highlands: 75th Annual GSA Meeting.
- Harangi, S., Downes, H., Thirlwall, M., and Gmeling, K., 2007, Geochemistry, petrogenesis and geodynamic relationships of Miocene calc-alkaline volcanic rocks in the western Carpathian arc, eastern central Europe: *Journal of Petrology*, v. 48, no. 12, p. 2261-2287.
- Irvine, T.N., and Baragar, W.R.A., 1971, A guide to the chemical classification of the common volcanic rocks: *Canadian Journal of Earth Sciences*, v. 8, p. 523-543.
- Kalczynski, M.J., Gates, A.E., Gorring, M.L., and Lupulescu, M.V., 2012, Hydrothermal alteration, mass transfer and magnetite mineralization in dextral shear zones, western Hudson Highlands, NY: Geological Society of America, Abstracts with Programs, v. 44, no. 2, p. 105.
- Kay, S.M., Ramos, V.A., and Kay, R.W., 1984, Elementos mayoritarios y trazas de las vulcanitas ordovicicas de la Precordillera Occidental: Basaltos de rift oceanico temprano proximas al margin continental, *in Actas 9th Congreso Geologico Argentino, Bariloche*, v. 8, p. 48-65.
- LeBas, M.J., LeMaitre, R.W., Streckeisen, A., and Zanettin, B., 1986, A chemical classification of volcanic rocks based on the total alkali-silica diagram: *Journal of Petrology*, v. 27, p. 745-750.

- Pearce, J.A., Harris, N.B.W., and Tindle, A.G., 1984, Trace element discrimination diagrams for the tectonic interpretation of granitic rocks: *Journal of Petrology*, v. 25, part 4, p. 956-983.
- Rollinson, H.R., 1993, *Using geochemical data: evaluation, presentation, interpretation*: Harlow, England: Pearson/Prentice Hall, p. 48-149.
- Rudnick, R.L. and Presper, T., 1990, Geochemistry of intermediate/-to high-pressure granulites: *Granulites and Crustal Evolution*, NATO Series, v. 311, p. 523-550.
- Sorenson, S.S., Grossman, J.N., and Perfit, M.R., 1997, Phengite-hosted LILE enrichment in eclogite and related rocks: implications for fluid-mediated mass transfer in subduction zones and arc magma genesis: *Journal of Petrology*, v. 38, iss. 1, p. 3-34.
- Volkert, R.A., 2004, Mesoproterozoic rocks of the New Jersey Highlands, north-central Appalachians: petrogenesis and tectonic history. *Geological Society of America: Memoir v. 197*, p. 697-728.
- Winter, J.D., 2010, *Principles of igneous and metamorphic petrology*, 2nd ed.: New York: Prentice Hall, p. 135-627.

APPENDIX A: FIGURES

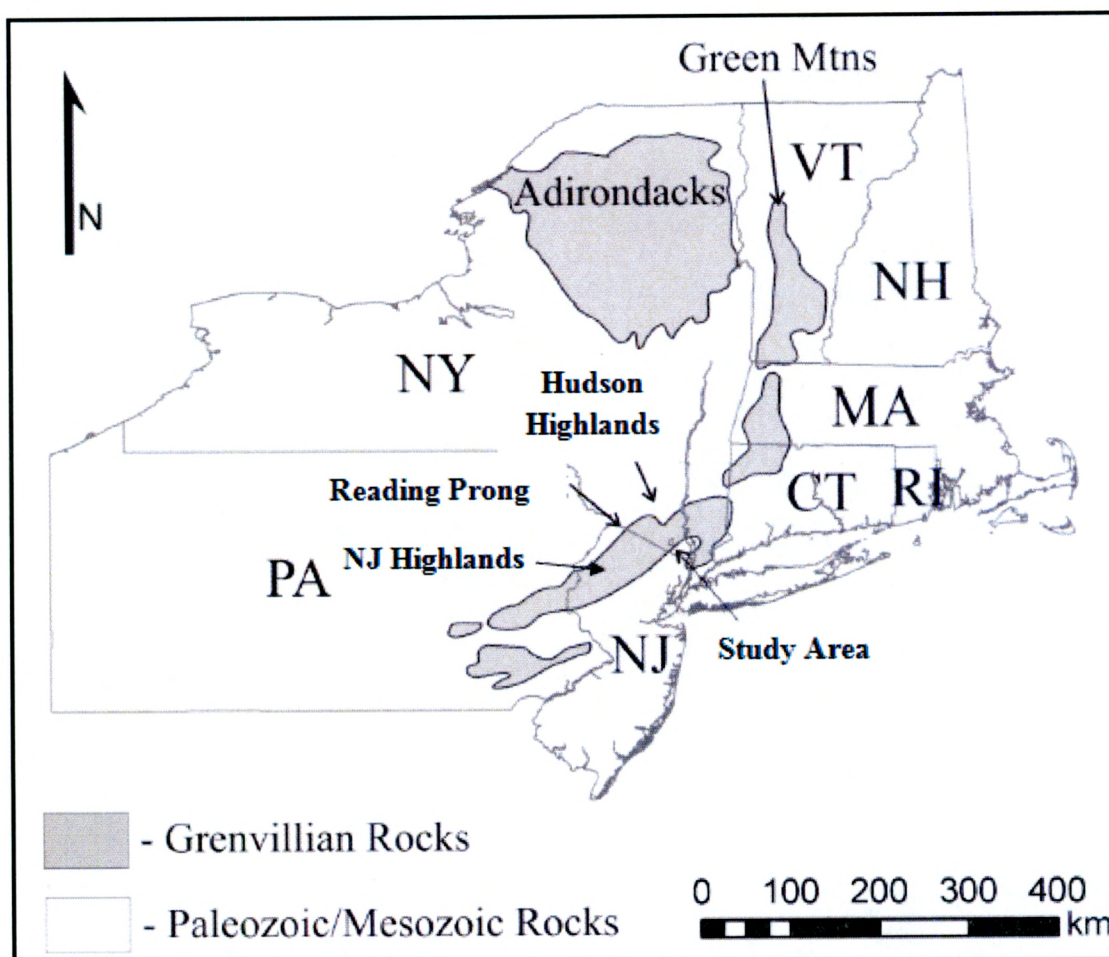
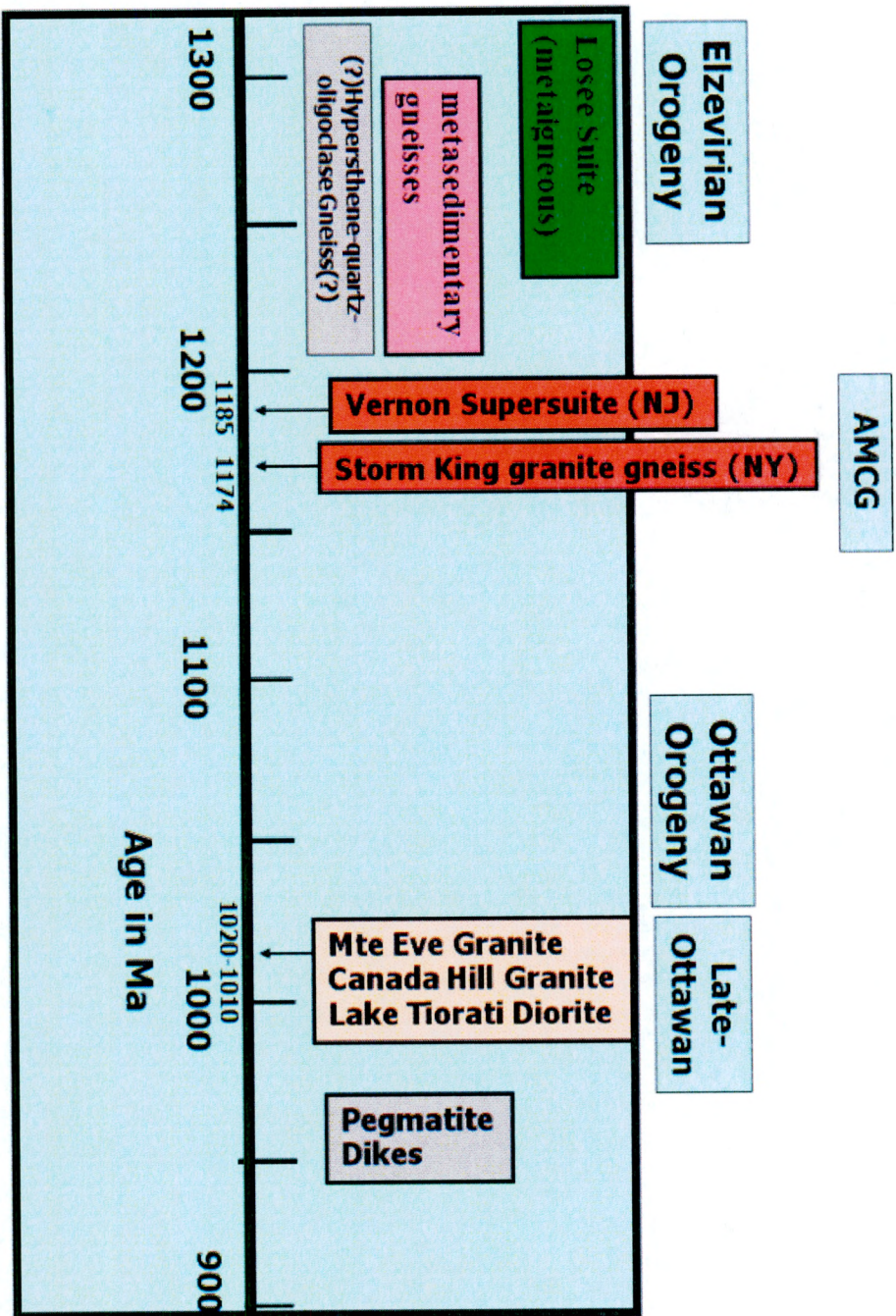


Figure 1. Generalized map of the northeastern United States illustrating the distribution of Grenvillian rocks, the Reading Prong, Hudson Highlands, New Jersey Highlands, and the study area (modified from Kalczynski *et al.*, 2012).

Figure 2. General geochronology of the Hudson Highlands and the New Jersey Highlands.



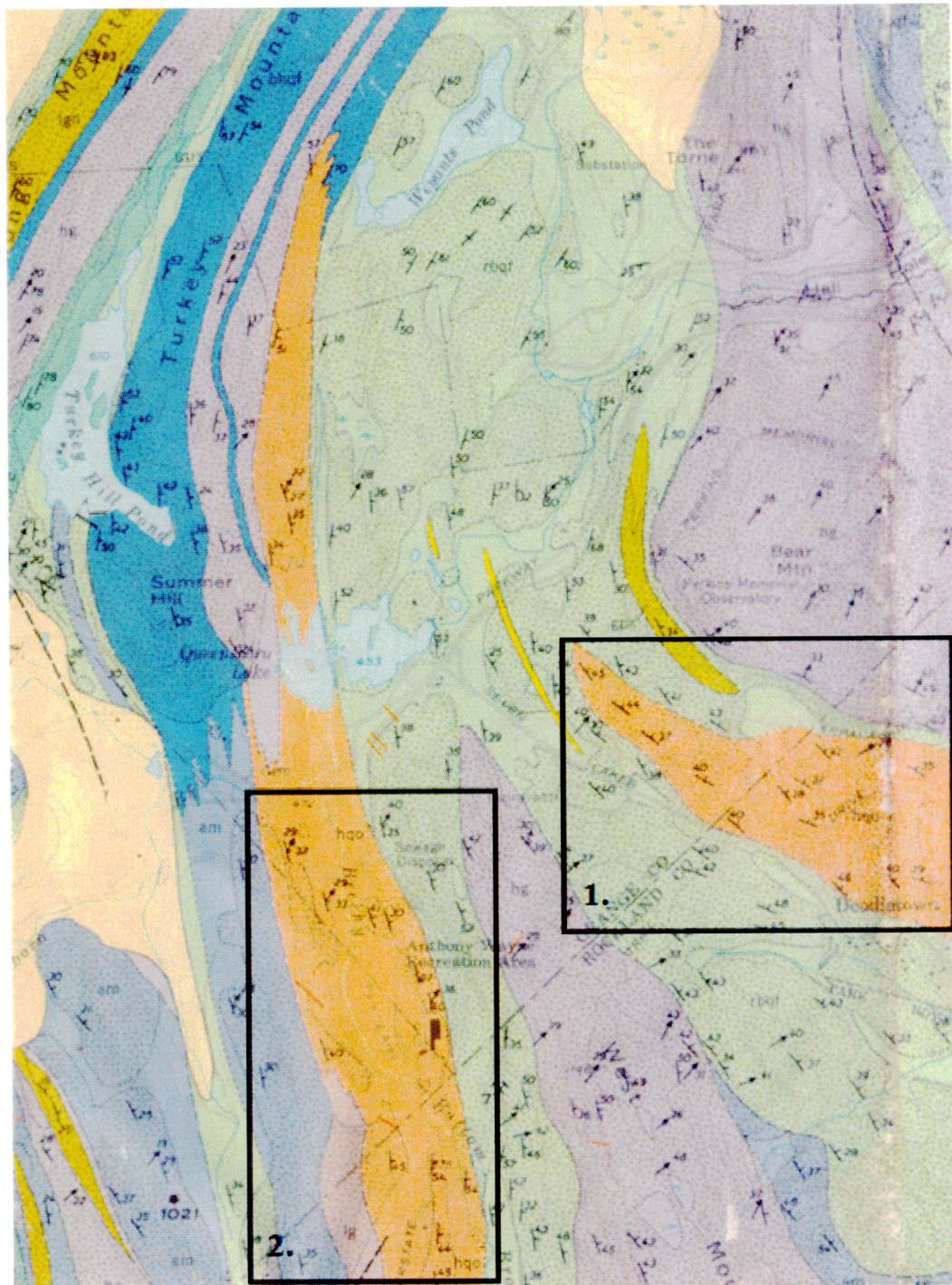


Figure 3. Geologic map of the sampling area from Dodd (1965). Orange color represents (Hqo) hypersthene-quartz-oligoclase gneiss. Boxes 1 and 2 are shown in more detail in Figure 4.

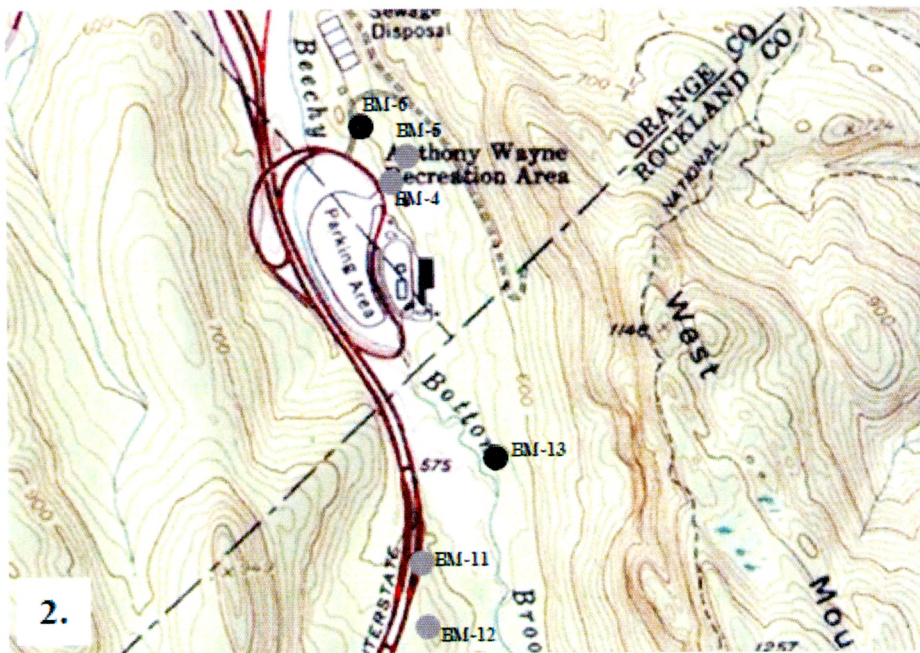
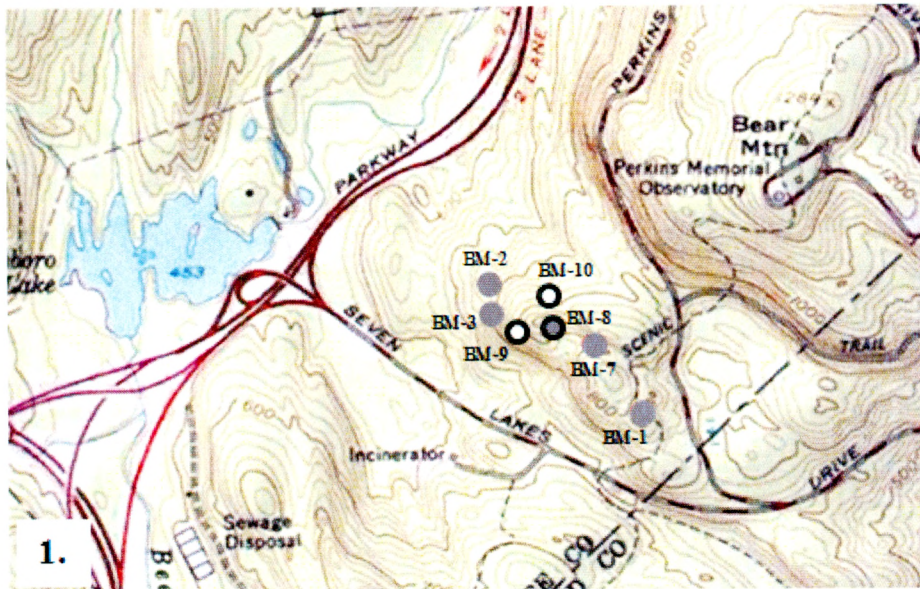


Figure 4. Sample location details on topographic map. Box 1 shows locations of BM-1, BM-2, BM-3, BM-7, BM-8(T, M, and B), BM-9, and BM-10. Box 2 shows the locations of BM-4, BM-5, BM-6, BM-11, BM-12, and BM-13. (ESRI 2011. ArcGIS Desktop: Release 10. Redlands, CA: Environmental Systems Research Institute).

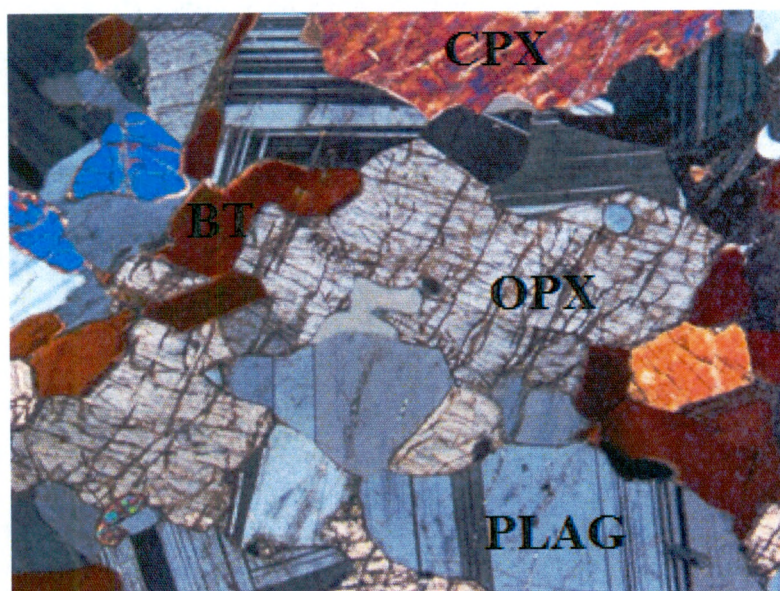
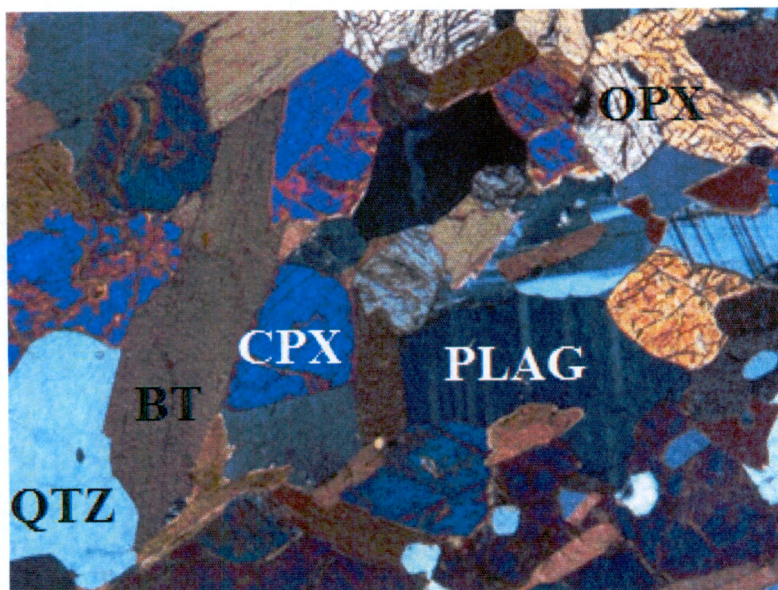


Figure 5. Thin section images in crossed polars (10x) of two hypersthene-quartz-oligoclase gneiss samples. Abbreviations are as follows: CPX clinopyroxene, OPX orthopyroxene, BT biotite, PLAG plagioclase feldspar, QTZ quartz. Top image was taken from BM-8-T and the bottom image was taken from BM-1.

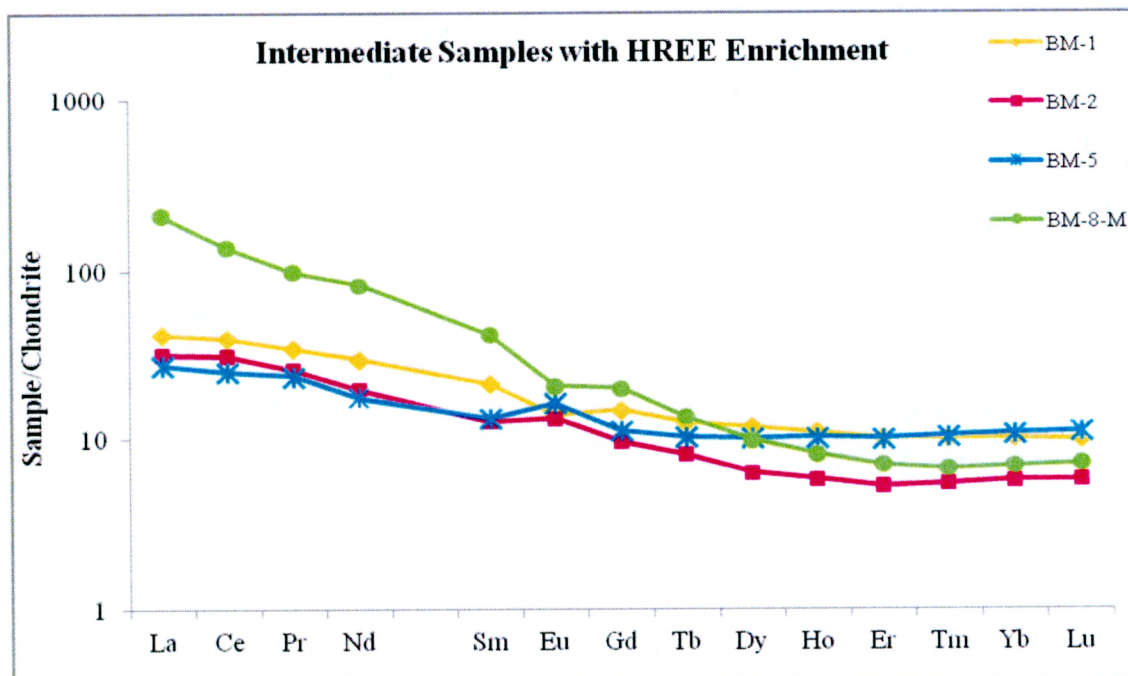
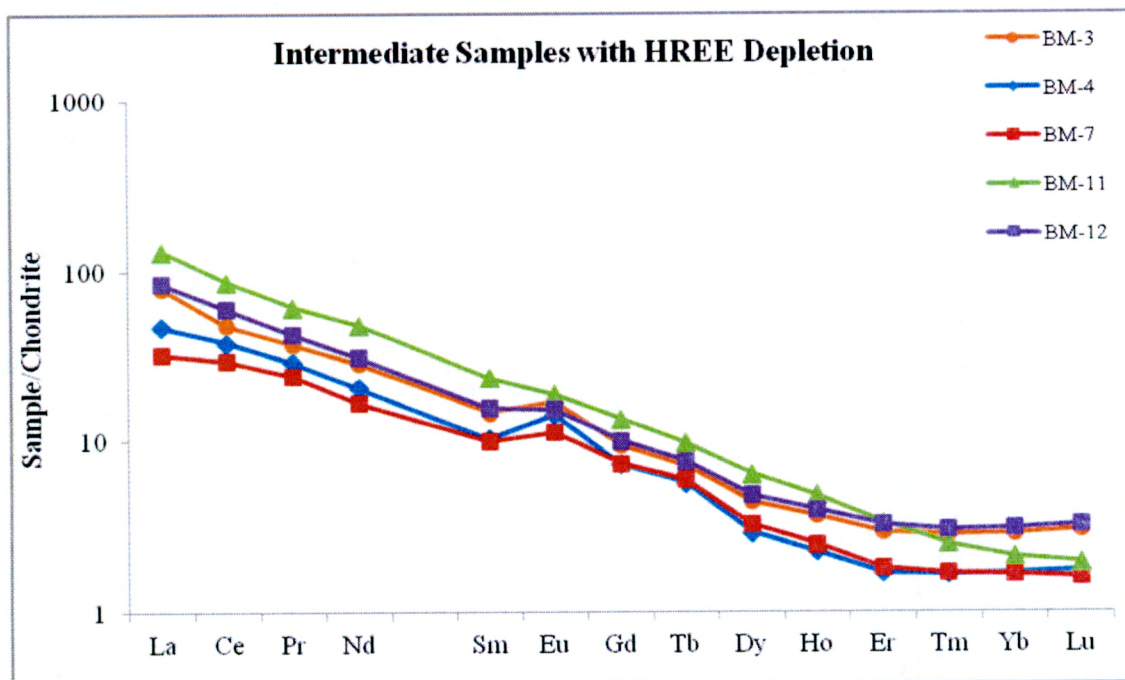


Figure 6. Chondrite-normalized REE patterns for the hypersthene-quartz-oligoclase gneiss. Samples are grouped according to SiO₂ content and HREE signature. Normalization factors are summarized in Table 16.

Continued on the following page.

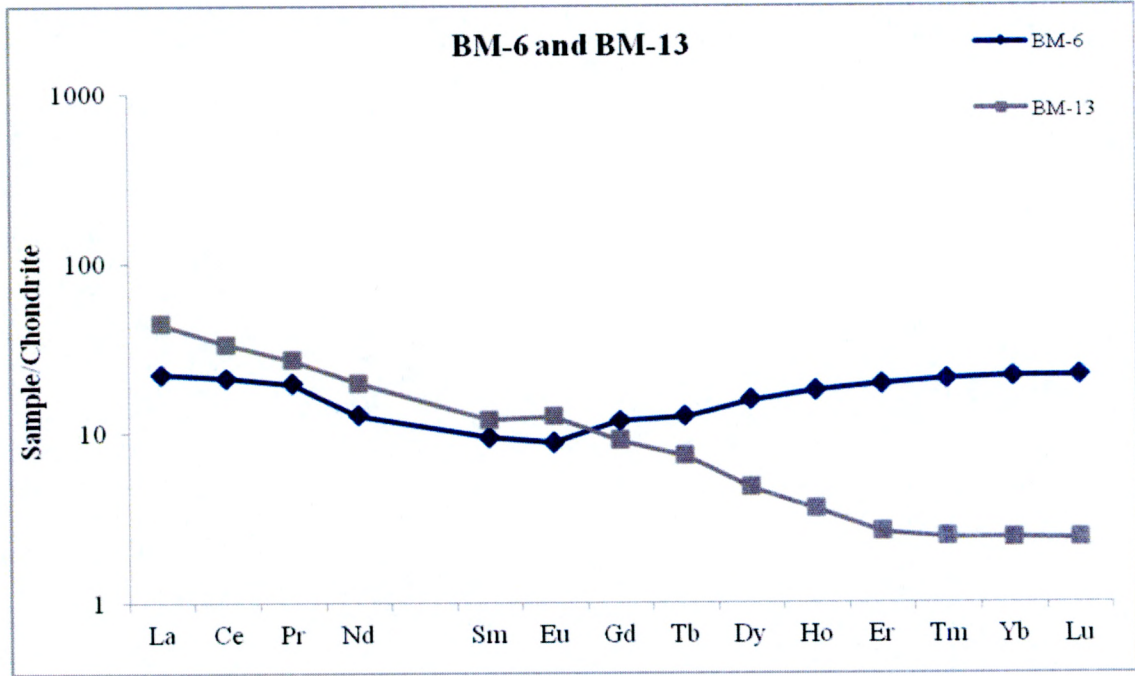
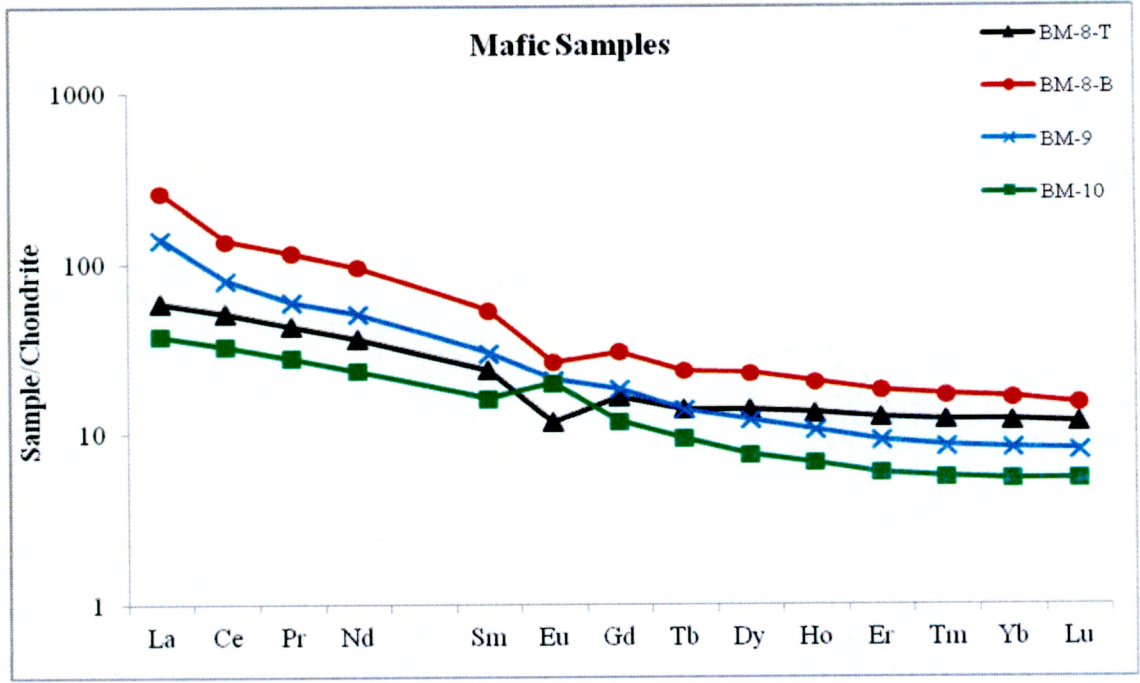


Figure 6. Continued.

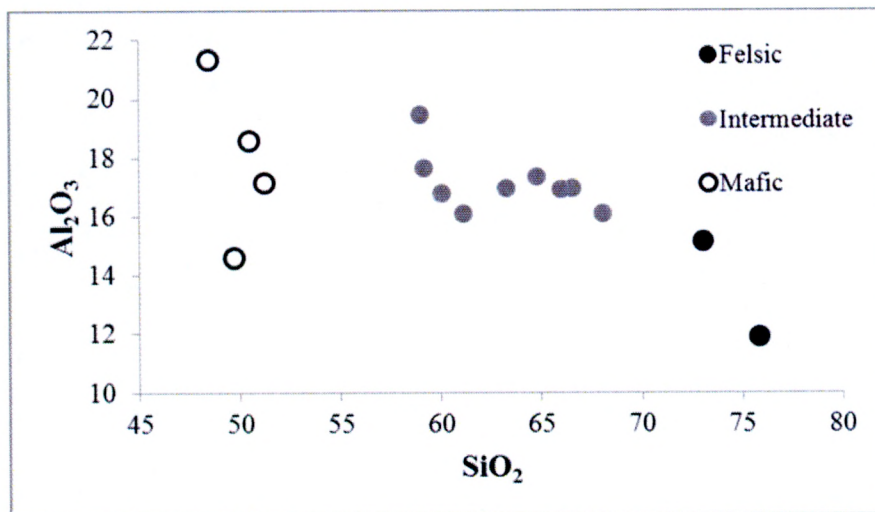
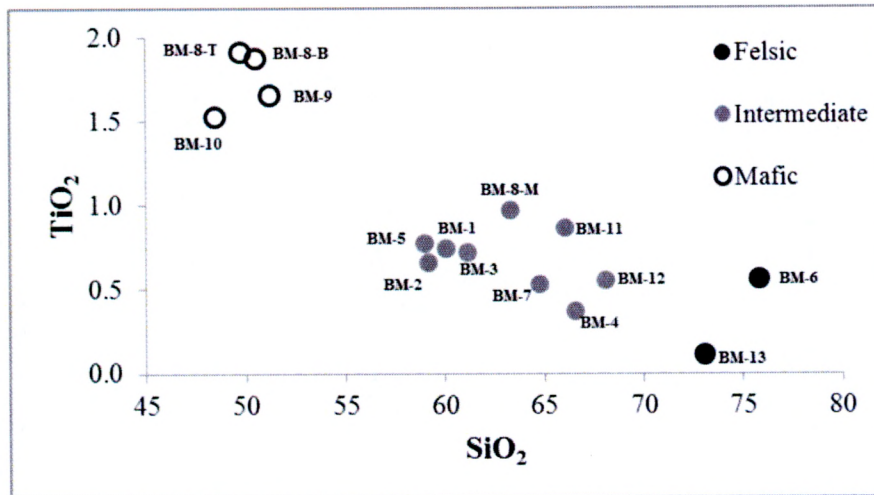


Figure 7. Harker diagrams for the hypersthene-quartz-oligoclase gneiss. Oxides are plotted in weight %. Geochemical data for the Losee Suite and metasedimentary rock samples plotted are taken from Drake and Volkert (1999). Geochemical data for hypersthene-quartz-oligoclase gneiss samples plotted are reported in Table 5.

Continued on following page.

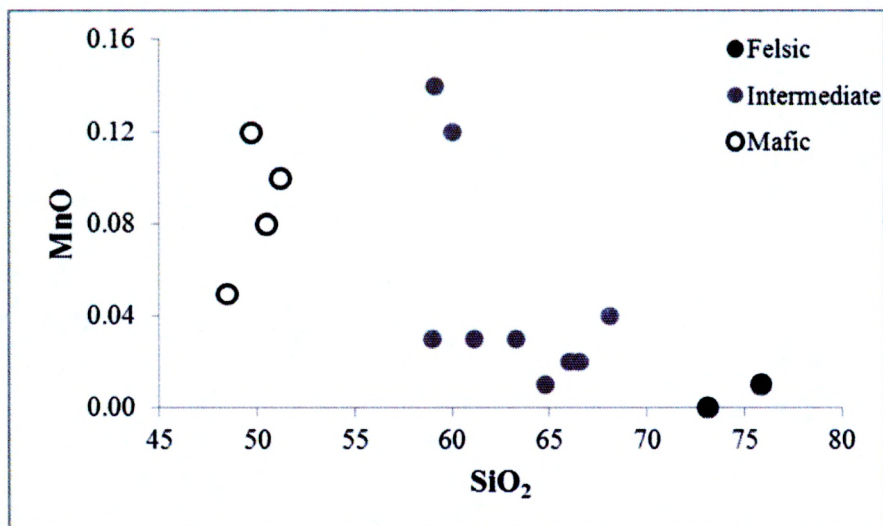
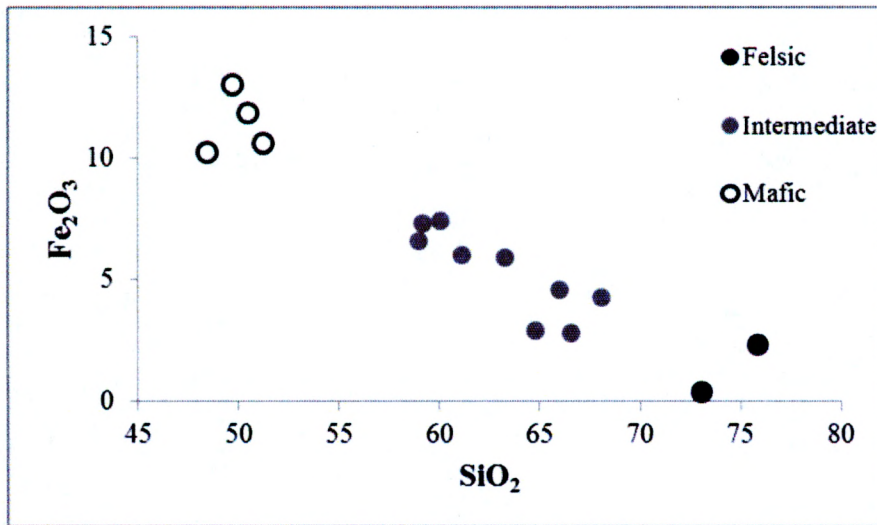


Figure 7. Continued

Continued on following page.

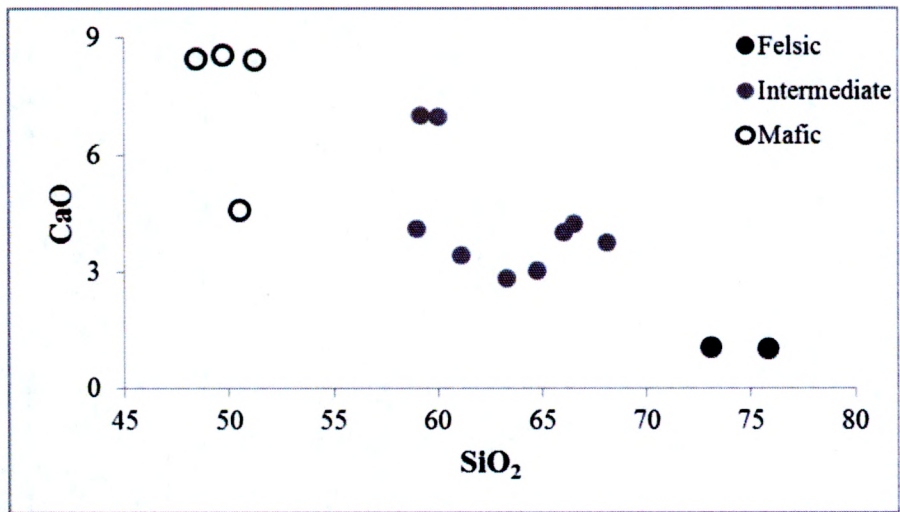
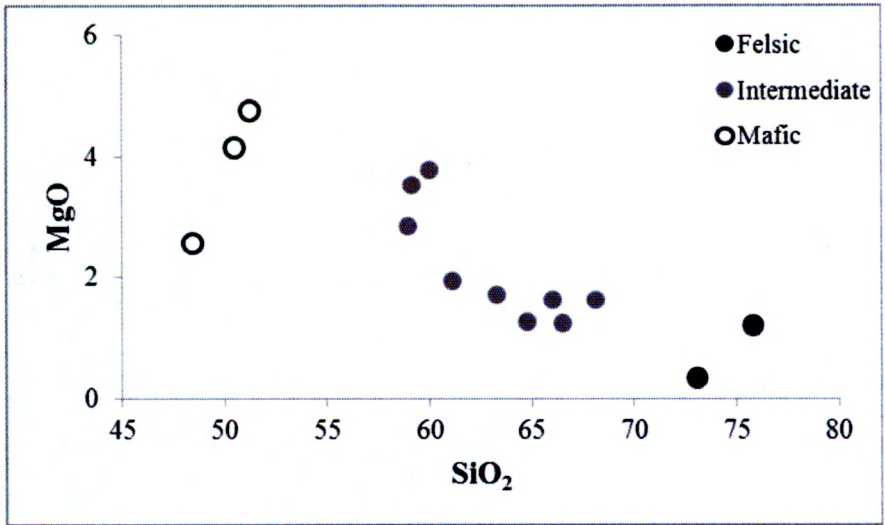


Figure 7. Continued

Continued on following page.

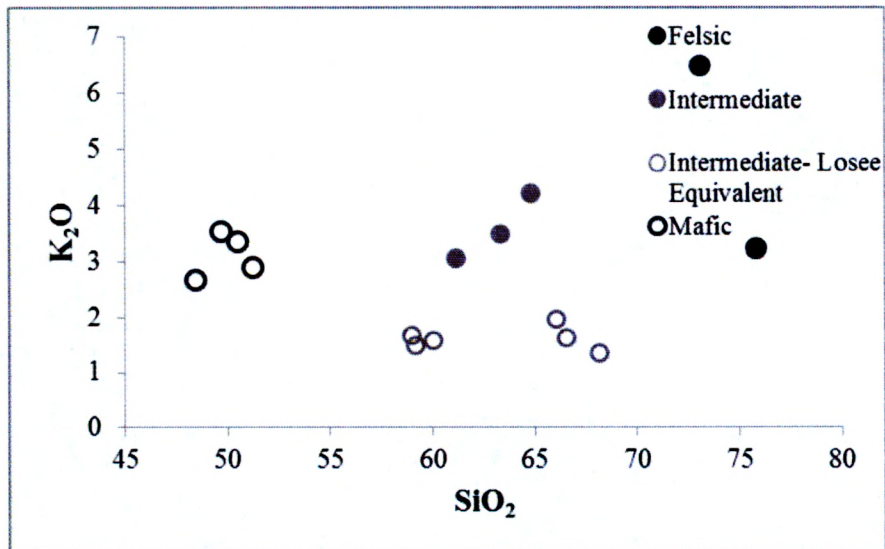
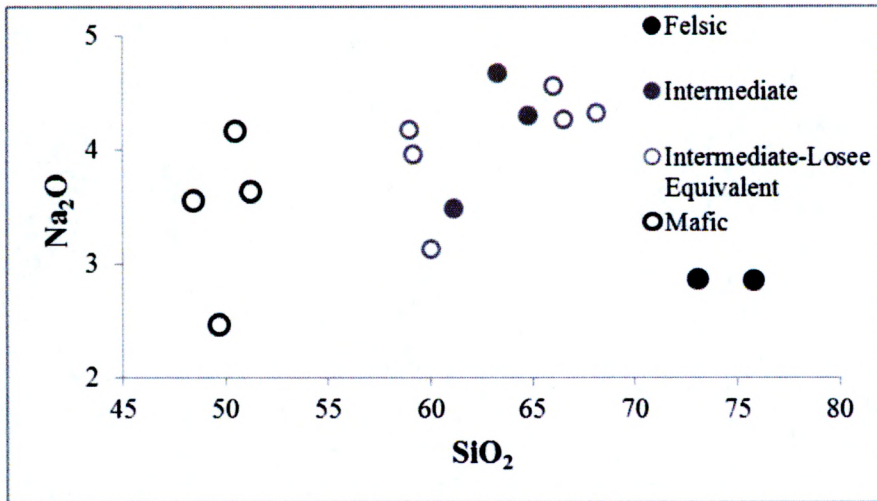


Figure 7. Continued

Continued on following page.

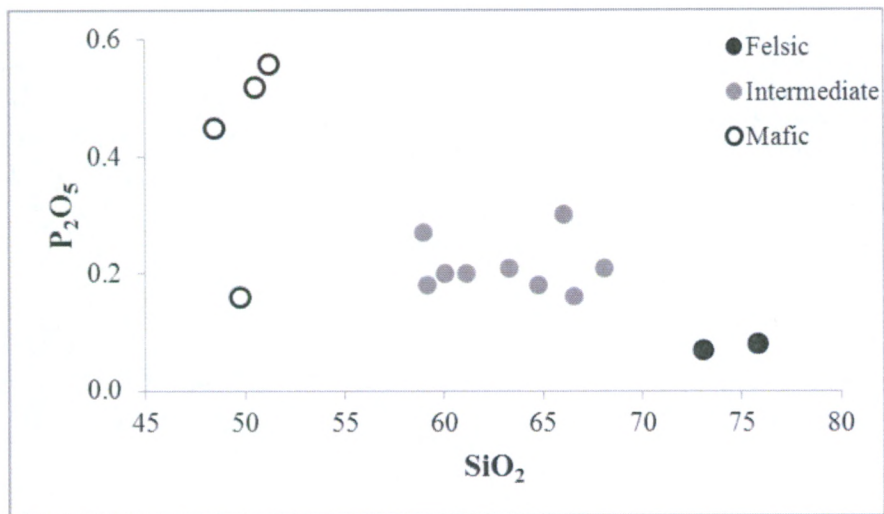


Figure 7. Continued.

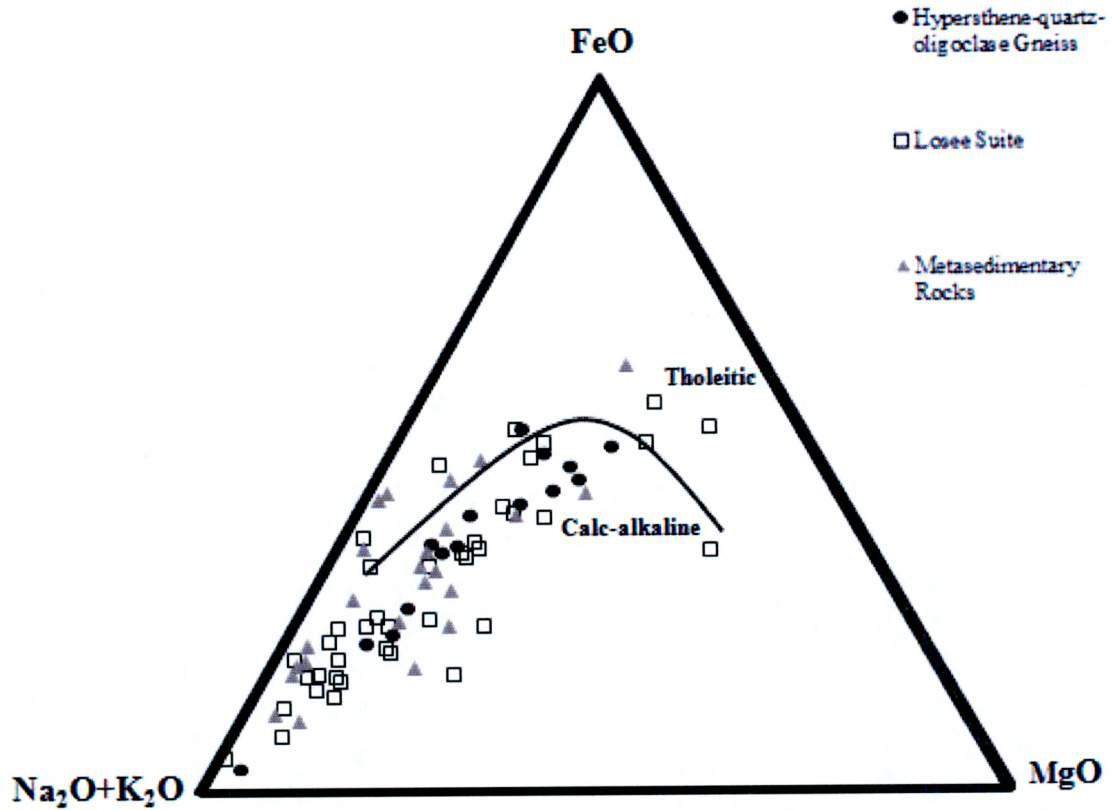


Figure 8. AFM diagram depicting selected compositions of the Losee Suite, metasedimentary rocks, and hypersthene-quartz-oligoclase gneiss. Geochemical data for the Losee Suite and metasedimentary rock samples plotted are taken from Drake and Volkert (1999). Geochemical data for hypersthene-quartz-oligoclase gneiss samples plotted are reported in Table 5. Line separating tholeiitic versus calc-alkaline series rocks provided by Irvine and Barager (1971).

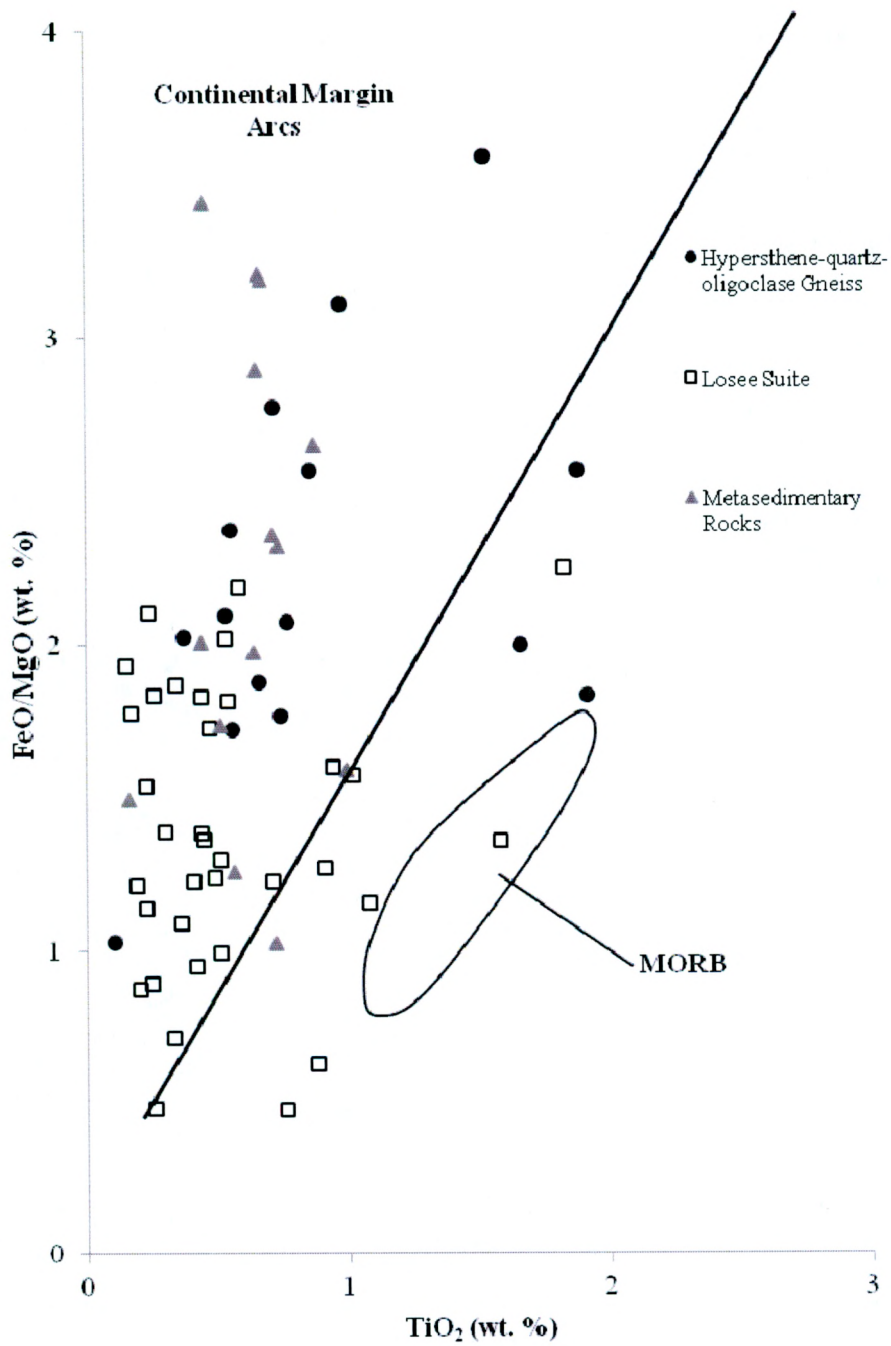


Figure 9. FeO/MgO versus TiO₂ plot (modified from Kay *et al.*, 1984) of Losee Suite, metasedimentary rocks, and hypersthene-quartz-oligoclase gneiss. Geochemical data for the Losee Suite and metasedimentary rock samples plotted are taken from Drake and Volkert (1999). Geochemical data for hypersthene-quartz-oligoclase gneiss samples plotted are reported in Table 5.

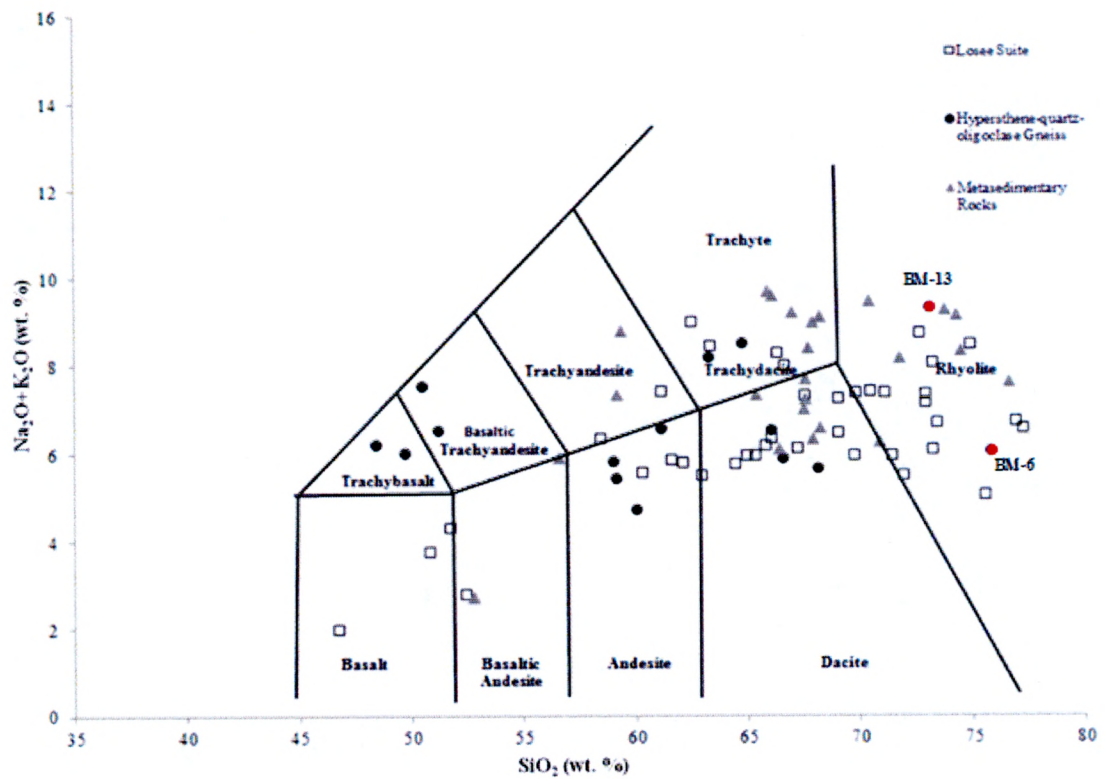


Figure 10. Total alkali-silica plot (modified from LeBas *et al.*, 1986) depicting selected compositions of the Losee Suite, metasedimentary rocks, and hypersthene-quartz-oligoclase gneiss. Red data points are labeled with corresponding sample name. Geochemical data for the Losee Suite and metasedimentary rock samples plotted are taken from Drake and Volkert (1999). Geochemical data for hypersthene-quartz-oligoclase gneiss samples plotted are reported in Table 5.

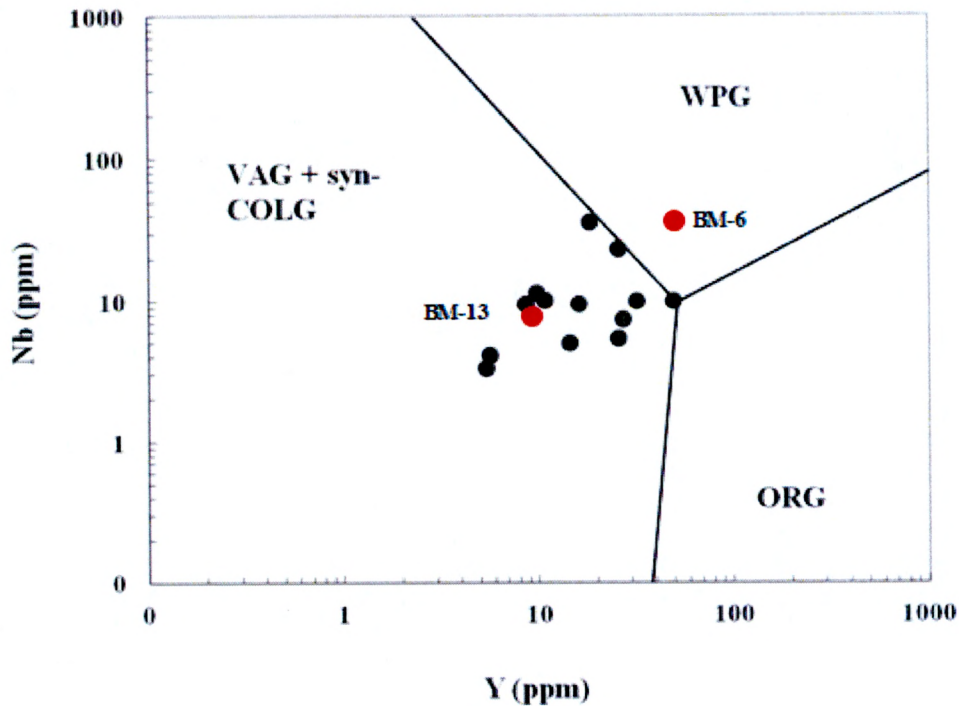
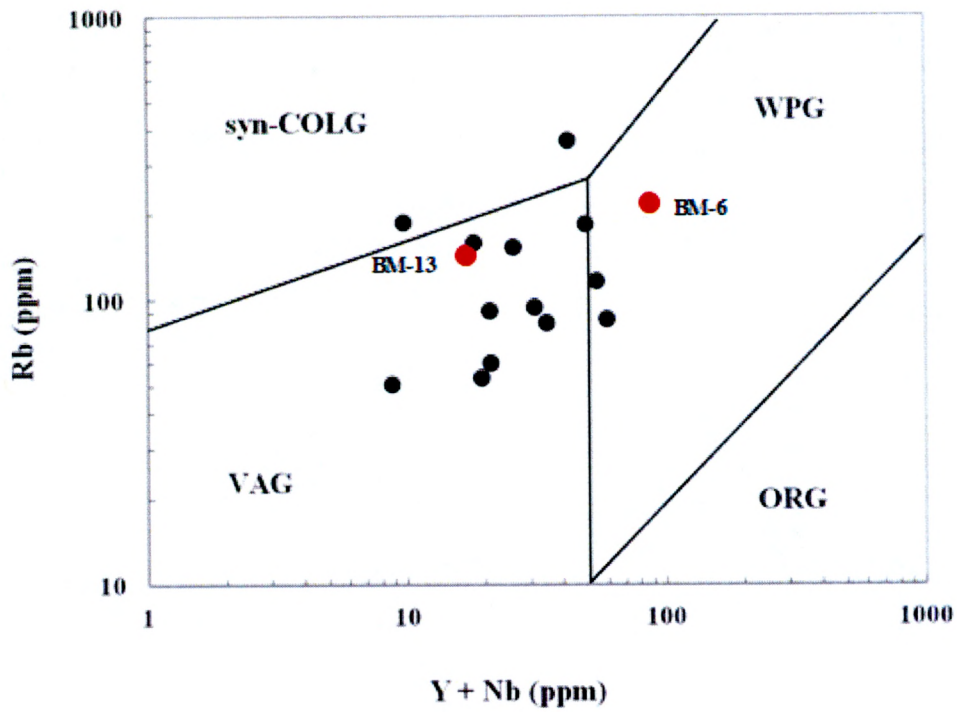


Figure 11. Nb, Rb, and Y tectonic discrimination diagrams of the hypersthene-quartz-oligoclase gneiss (modified from Pearce *et al.*, 1984). Fields of tectonic settings are as follows: syn-COLG is syn-collision granite, VAG is volcanic arc granite, WPG is within plate granite, and ORG is oceanic ridge granite. Red data points are labeled with corresponding sample name.

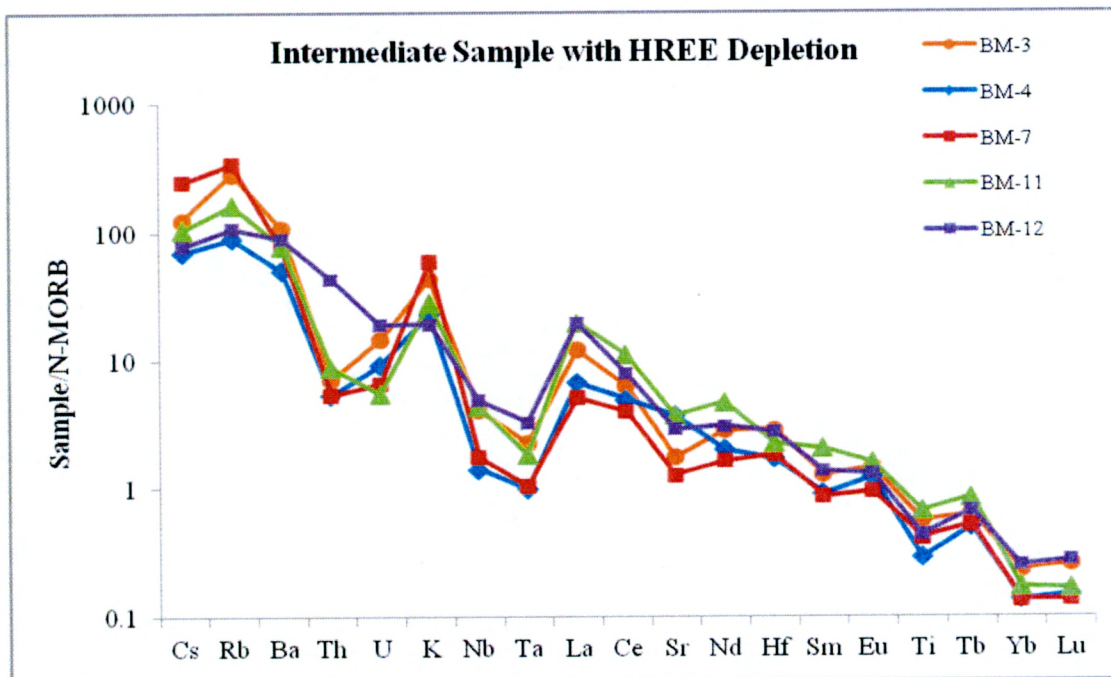
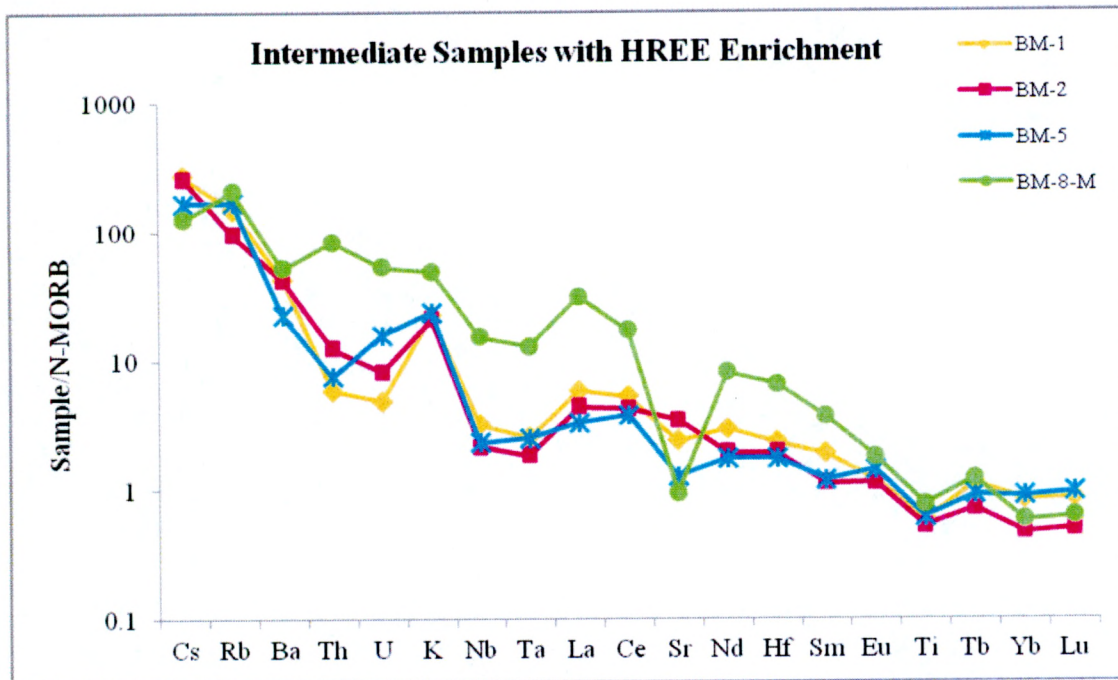


Figure 12. N-MORB-normalized multi-element diagrams for the hypersthene-quartz-oligoclase gneiss. Samples grouped according to SiO₂ content and HREE signature. Normalization factors are summarized in Table 16.

Continued on the following page.

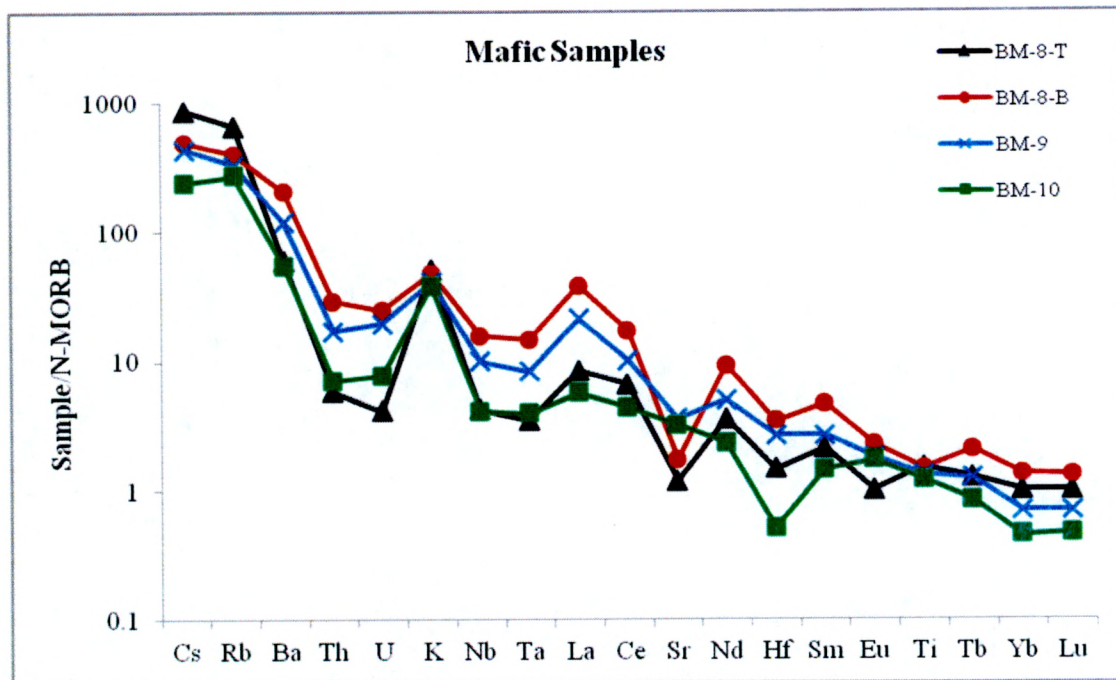


Figure 12. Continued.

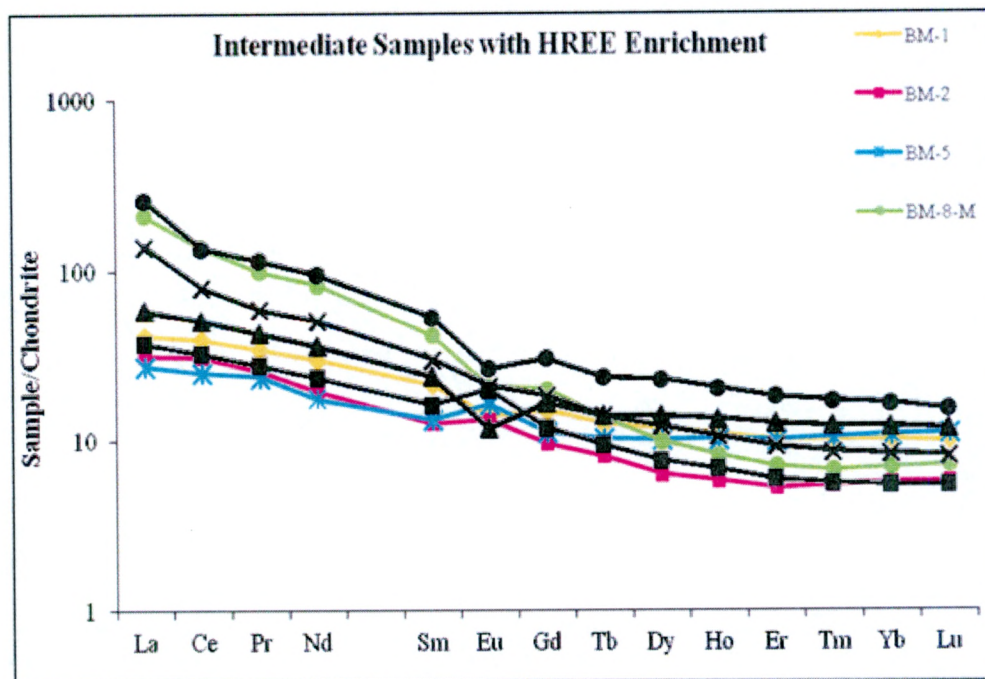
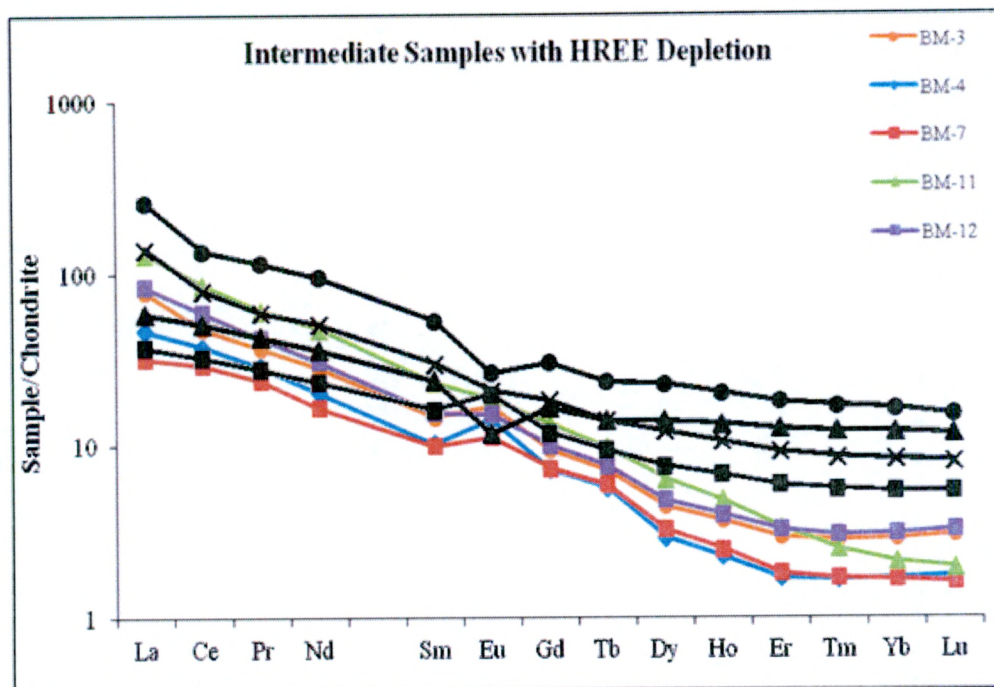


Figure 13. Comparisons of REE plot patterns between mafic samples considered to be “parent” compositions (black lines) and the intermediate samples representative of potential “daughter” compositions of the hypersthene-quartz-oligoclase gneiss.

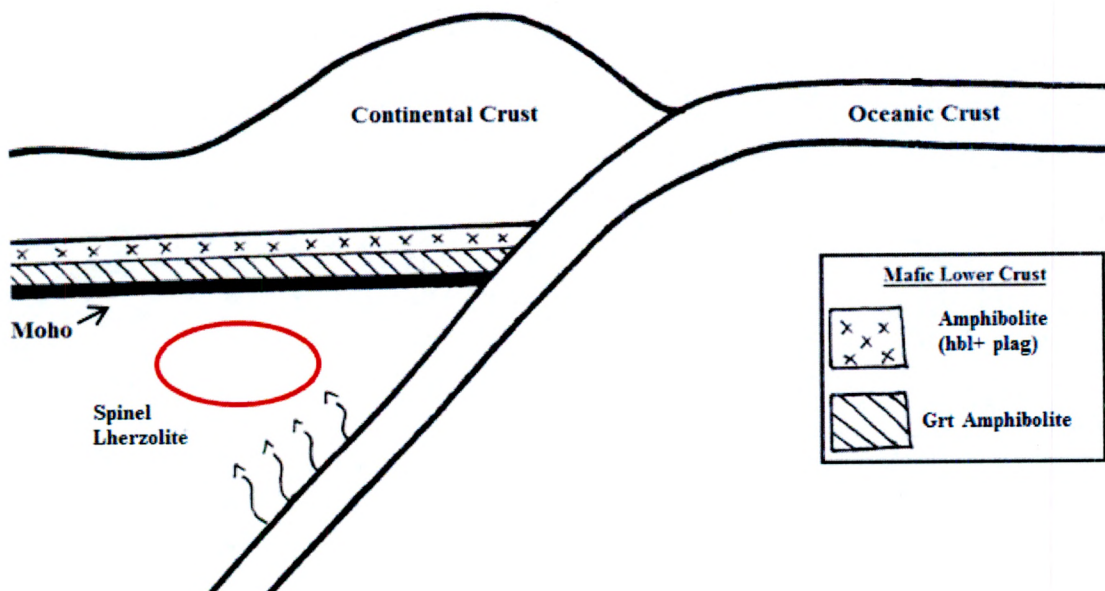


Figure 14. Graphic representation of the location of magma generation for the mafic composition samples of the hypersthene-quartz-oligoclase gneiss. The red circle indicates the general area of melting.

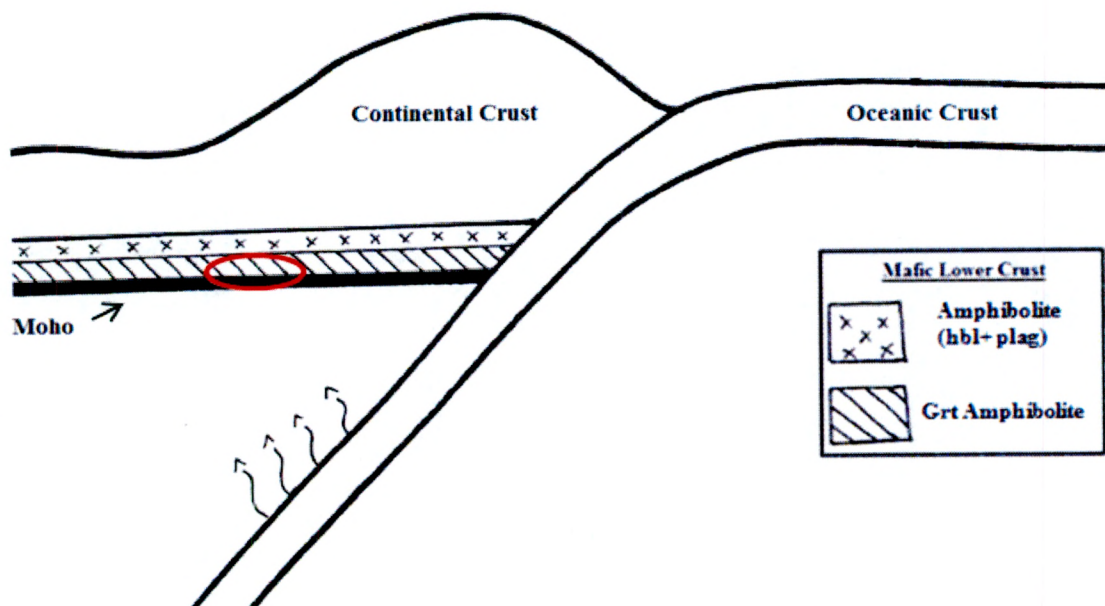


Figure 15. Graphic representation of the location of magma generation for the intermediate composition samples with HREE depletion of the hypersthene-quartz-oligoclase gneiss. The red circle indicates the general area of melting.

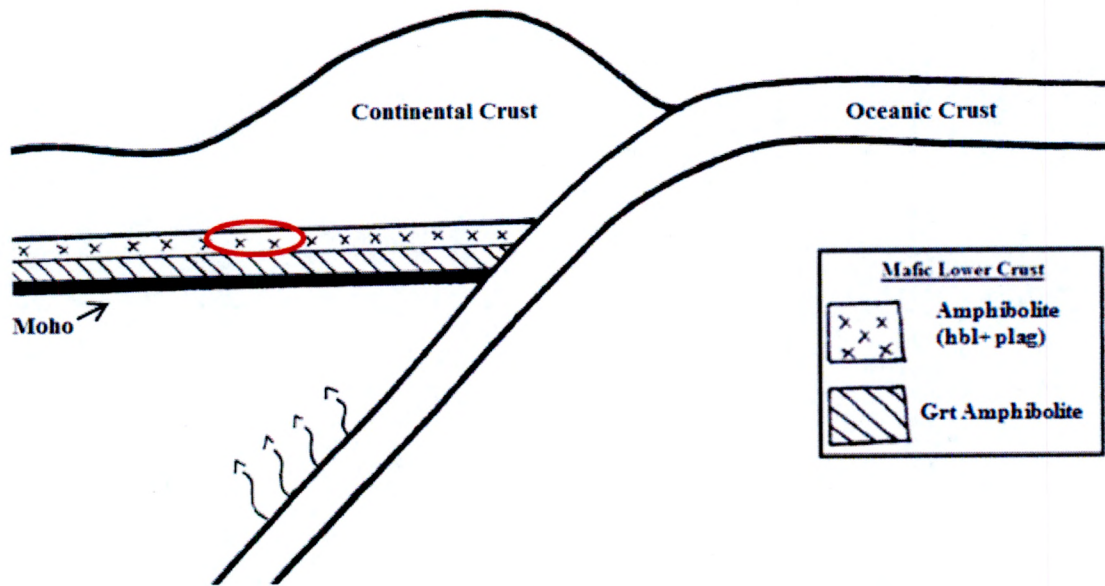


Figure 16. Graphic representation of the location of magma generation for the intermediate composition samples with HREE depletion of the hypersthene-quartz-oligoclase gneiss. The red circle indicates the general area of melting.

APPENDIX B: TABLES

Table 1. Field observations, locations, and hand sample descriptions of the hypersthene quartz-oligoclase gneiss from the Hudson Highlands, NY.

Sample	GPS Coordinates	Description
BM-1	41°18.338 N 74°00.709 W	Fine to medium grained light grey gneiss. Outcrop is a small knob located along the western side of the AT trail north of Seven Lakes Drive. Strike: S20°E, dip: 42°NE.
BM-2	41°18.500 N 74°01.020 W	Fine to medium grained grey gneiss altered to light brown in some areas. Outcrop is close to the contact with rusty biotite-quartz-feldspar gneiss. Strike: S33°E, dip: 40°NE.
BM-3	41°18.540 N 74°01.030 W	Medium grained grey-tan gneiss in which altered brown hypersthene can be seen in hand sample. Outcrop is close to the contact with rusty biotite-quartz-feldspar gneiss. Strike: S27°E, dip: 53°NE.
BM-4	41°17.897 N 74°01.561 W	Fine to medium grained grey gneiss altered to brown on some surfaces. Outcrop is located at the entrance of the Anthony Wayne Recreation Area's main parking lot. Strike: N10°W, dip: 31°E.
BM-5	41°17.933 N 74°01.535 W	Fine grained grey gneiss altered to red-brown on some surfaces. Outcrop is located close to the entrance of the Anthony Wayne Recreation Area's main parking lot and northeast of BM-4. Strike: N15°W, dip: 35°E.
BM-6	41°17.985 N 74°01.623 W	Fine grained grey gneiss altered to brown on some surfaces with well defined banding. Outcrop is located east of the gravel trail starting at the entrance of the Anthony Wayne Recreation Area's main parking lot. Strike: N11°W, dip: E 32°.
BM-7	41°18.445 N 74°00.814 W	Fine grained grey-tan gneiss altered to brown on some surfaces. Outcrop is close to contact with rusty biotite-quartz-feldspar gneiss which is to the north. Strike: N60°W, dip: 35°E.
BM-8-T BM-8-M BM-8-B	41°18.470 N 74°00.895 W	Three samples were collected from this outcrop as it was one of the larger and more easily accessible exposures. BM-8-T was collected from the top of the exposure, 8-M from the middle, and 8-B from the base. Hypersthene is easily identifiable in all hand samples, with the largest grains found in 8-T and 8-M. All samples are fine to medium grained grey gneiss that is altered to a dark grey-brown. 8-T and 8-B appear to be comprised of slightly more mafic minerals than 8-M. Additionally, minor amounts of hornblende are seen in hand sample of 8-B. Strike: N30°W, dip: 34°E.
BM-9	41°18.462 N 74°00.974 W	Medium grained grey gneiss altered to dark grey-brown. Small pyroxene grains are identifiable in hand-sample. No strike or dip was taken at this location.
BM-10	41°18.522 N 74°00.910 W	Medium grained light grey gneiss with minor alteration on exposed surfaces. Strike: N37°W, dip: 40°E.
BM-11	41°17.309 N 74°01.512 W	Medium grained grey-tan gneiss abundant in quartz and plagioclase. Outcrop located along the eastern side of the Palisades Interstate across from the book store. Strike: N15°E, dip: 42°E.
BM-12	41°17.202 N 74°01.492 W	Medium grained grey gneiss. Outcrop located just south of BM-11. Strike: N12°W, dip: 40°E.
BM-13	41°17.470 N 74°01.345 W	Fine grained light grey gneiss abundant in felsic minerals. Outcrop located along Bottom Brook south of the Anthony Wayne Recreation Area. Strike: N15°E, dip: 41°E.

Table 2. Modal Analysis of the hypersthene-quartz-oligoclase gneiss.

Sample	BM-1	BM-2	BM-3	BM-4	BM-5	BM-6	BM-7	BM-8-T	BM-8-M	BM-8-B	BM-9	BM-10	BM-11	BM-12	BM-13
Plagioclase	60	68	53	54	66	5	43	48	30	49	47	69	68	59	3
Potash Feldspar	0	0	1	0	0	45	29	17	44	20	3	0	2	2	52
Quartz	20	14	36	39	21	56	22	5	17	7	12	4	24	35	41
Hornblende	0	0	0	0	0	0	0	0	0	1	12	8	0	0	0
Biotite	8	6	6	4	9	24	4	15	2	12	10	9	3	3	2
Clinopyroxene	3	3	0	0	0	0	0	8	0	1	7	0	0	0	0
Orthopyroxene	7	5	3	1	0	0	0	7	4	5	5	0	3	0	0
Garnet	0	0	0	0	2	0	0	0	0	0	0	2	0	0	0
Opagues	tr	1	tr	tr	tr	tr	0	0	2	3	1	1	tr	0	tr
Zircon	0	0	tr	tr	tr	tr	0	0	0	tr	0	0	tr	0	tr
Alteration	2	3	1	2	2	0	2	tr	1	2	3	7	0	1	2

Table 3. Summary of ICP-OES reproducibility. Element averages are expressed in weight %. Averages and RSD values are based on 8 sample preparations.

Un-normalized Values									
Element	BM-11			AGV-2	AGV-2				
	Average	StDev	% RSD		Average	StDev	% RSD	Accuracy	
SiO ₂	66.98	0.38	0.56	59.30	60.37	0.89	1.47	1.80	
TiO ₂	0.86	0.02	2.01	1.05	1.05	0.02	1.82	0.12	
Al ₂ O ₃	14.62	0.11	0.79	16.91	16.94	0.28	1.68	0.16	
Fe ₂ O ₃	4.01	0.07	1.72	6.69	6.85	0.12	1.72	2.32	
MnO	0.02	0.00	6.85	0.09	0.10	0.00	2.98	7.96	
MgO	1.57	0.03	1.78	1.79	1.80	0.03	1.69	0.55	
CaO	3.99	0.05	1.22	5.20	5.22	0.09	1.75	0.33	
Na ₂ O	4.66	0.04	0.93	4.19	4.21	0.08	1.96	0.58	
K ₂ O	1.99	0.04	1.89	2.88	2.93	0.07	2.45	1.57	
P ₂ O ₅	0.28	0.01	3.40	0.48	0.48	0.01	2.61	0.38	
Total	101.63	0.63	0.62	98.58	99.94	1.56	1.57	1.37	

Normalized Values									
Element	BM-11			AGV-2	AGV-2				
	Average	StDev	% RSD		Average	StDev	% RSD	Accuracy	
SiO ₂	66.98	0.38	0.16	60.15	60.41	0.09	0.16	0.42	
TiO ₂	0.86	0.02	0.34	1.07	1.05	0.00	0.34	1.48	
Al ₂ O ₃	14.62	0.11	0.44	17.15	16.95	0.07	0.44	1.20	
Fe ₂ O ₃	4.01	0.07	0.29	6.79	6.85	0.02	0.29	0.93	
MnO	0.02	0.00	1.75	0.09	0.10	0.00	1.75	6.49	
MgO	1.57	0.03	0.33	1.82	1.80	0.01	0.33	0.81	
CaO	3.99	0.05	0.61	5.27	5.22	0.03	0.61	1.04	
Na ₂ O	4.66	0.04	0.95	4.25	4.22	0.04	0.95	0.78	
K ₂ O	1.99	0.04	1.12	2.92	2.98	0.03	1.12	0.18	
P ₂ O ₅	0.28	0.01	1.82	0.49	0.48	0.01	1.82	0.97	
Total	100.00	0.00	0.00	100.00	100.00	0.00	0.00	0.00	

Table 4. Summary of ICP-MS reproducibility. Element averages are expressed in ppm. Scandium values measured for AGV-2 are taken from the ICP-OES. Averages and RSD values are based on 8 sample preparations.

Un-normalized Values									
Element	BM-11			AGV-2					
	Average	StDev	% RSD	AGV-2	Average	StDev	% RSD	Accuracy	
Sc	18.93	2.27	12.00	13.00	13.09	0.83	6.34	0.67	
V	51.51	0.92	1.78	120.00	119.09	3.54	2.98	0.76	
Cr	20.45	1.16	5.66	17.00	21.45	2.26	10.56	26.15	
Co	10.16	0.29	2.86	16.00	15.98	0.64	3.98	0.12	
Ni	14.37	0.81	5.62	19.00	20.96	1.14	5.44	10.31	
Ga	21.71	0.20	0.93	20.00	20.44	0.31	1.53	2.22	
Rb	90.93	1.77	1.95	68.60	68.70	0.75	1.09	0.15	
Sr	491.80	6.56	1.33	658.00	690.02	10.37	1.50	4.87	
Y	10.41	0.30	2.90	20.00	22.35	2.28	10.19	11.73	
Zr	206.43	8.92	4.32	230.00	222.98	2.57	1.15	3.05	
Nb	10.37	0.21	2.03	15.00	14.36	0.42	2.90	4.24	
Cs	1.05	0.25	24.17	1.16	1.42	0.26	17.94	22.84	
Ba	502.38	19.37	3.86	1140.00	1135.26	12.15	1.07	0.42	
La	52.41	5.24	9.99	38.00	43.67	1.58	3.62	14.93	
Ce	80.31	1.48	1.84	68.00	63.86	0.51	0.80	6.09	
Pr	8.80	0.19	2.16	8.30	7.59	0.08	1.01	8.52	
Nd	33.79	0.67	1.97	30.00	30.46	0.27	0.88	1.53	
Sm	5.29	0.11	2.02	5.70	5.72	0.06	1.12	0.30	
Eu	1.63	0.03	1.89	1.54	1.63	0.02	1.31	5.77	
Gd	4.09	0.25	6.16	4.73	4.66	0.05	0.99	1.46	
Tb	0.56	0.01	2.34	0.64	0.68	0.00	0.65	5.57	
Dy	2.45	0.06	2.41	3.60	3.59	0.04	1.06	0.16	
Ho	0.41	0.01	2.69	0.71	0.70	0.01	1.14	1.95	
Er	0.82	0.02	2.64	1.79	1.77	0.02	1.21	0.99	
Tm	0.10	0.00	4.02	0.26	0.26	0.00	1.52	1.24	
Yb	0.53	0.02	2.93	1.60	1.64	0.02	1.43	2.58	
Lu	0.07	0.00	5.72	0.25	0.26	0.00	1.59	2.57	
Hf	4.88	0.27	5.45	5.08	5.06	0.14	2.79	0.46	
Ta	0.25	0.01	3.50	0.89	0.92	0.01	0.92	3.05	
Pb	12.22	4.17	34.09	37.27	16.17	1.99	12.30	56.63	
Th	0.73	0.43	59.79	6.10	6.13	0.26	4.19	0.57	
U	0.28	0.02	8.95	1.88	1.73	0.22	12.56	7.91	

Table 5. Whole-rock geochemistry of hypersthene-quartz-oligoclase gneiss.

Sample	BM-1	BM-2	BM-3	BM-4	BM-5	BM-6	BM-7	BM-8-T	BM-8-M	BM-8-B	BM-9	BM-10	BM-11	BM-12	BM-13
Major Elements (wt %)															
SiO ₂	60.02	59.14	61.10	66.53	58.97	75.82	64.76	49.67	63.28	50.44	51.17	48.40	66.01	68.09	73.09
TiO ₂	0.74	0.66	0.72	0.37	0.77	0.56	0.53	1.92	0.97	1.88	1.66	1.53	0.86	0.55	0.11
Al ₂ O ₃	16.78	17.63	16.11	16.95	19.46	11.89	17.35	14.63	16.97	18.58	17.15	21.38	16.92	16.07	15.12
Fe ₂ O ₃	7.46	7.36	6.02	2.79	6.59	2.32	2.93	13.09	5.94	11.91	10.63	10.27	4.61	4.29	0.39
MnO	0.12	0.14	0.03	0.02	0.03	0.01	0.01	0.12	0.03	0.08	0.10	0.05	0.02	0.04	0.00
MgO	3.79	3.53	1.95	1.24	2.86	1.21	1.26	6.42	1.72	4.17	4.78	2.57	1.62	1.63	0.34
CaO	7.00	7.02	3.42	4.26	4.12	1.02	3.05	8.59	2.86	4.62	8.46	8.50	4.03	3.77	1.05
Na ₂ O	3.14	3.97	3.50	4.27	4.18	2.85	4.31	2.47	4.68	4.17	3.64	3.56	4.56	4.33	2.86
K ₂ O	1.59	1.49	3.07	1.62	1.67	3.23	4.22	3.55	3.50	3.37	2.90	2.68	1.97	1.36	6.48
P ₂ O ₅	0.20	0.18	0.20	0.16	0.27	0.08	0.18	0.16	0.21	0.52	0.56	0.45	0.30	0.21	0.07
Total	100.84	101.11	96.12	98.20	98.91	98.97	98.59	100.62	100.16	99.73	101.06	99.40	100.88	100.33	99.51
Trace Elements (ppm)															
Sc	22.57	19.93	20.22	20.61	19.86	26.14	22.83	30.54	18.47	18.37	20.16	18.58	21.17	20.97	26.68
V	93.00	99.02	68.73	40.22	48.95	54.69	42.10	333.33	62.29	210.54	215.72	197.23	52.76	57.20	11.31
Cr	62.43	17.83	38.31	12.35	10.42	31.47	10.41	126.42	18.62	83.56	167.20	23.09	21.64	19.96	7.99
Co	13.68	18.47	10.44	5.05	7.19	2.34	2.63	23.36	14.48	18.81	37.37	14.97	10.38	9.37	1.83
Ni	10.14	6.12	12.63	9.84	8.89	6.22	7.67	73.45	12.91	30.05	97.83	8.10	13.81	11.36	7.85
Ga	18.18	18.72	19.85	20.69	21.91	13.95	19.04	21.89	21.35	25.64	22.58	22.74	21.88	20.91	18.61
Rb	83.45	53.37	159.37	50.60	94.79	86.05	187.71	366.69	116.54	221.80	185.92	153.57	91.92	60.19	147.43
Sr	319.09	463.17	235.59	501.60	169.89	107.93	170.76	157.53	125.78	235.35	490.10	432.19	500.39	391.62	213.09
Y	27.29	14.46	8.61	5.40	25.77	49.59	5.61	32.15	18.41	49.43	25.77	16.22	10.80	9.78	9.12
Zr	188.96	157.56	236.21	145.39	149.35	279.78	166.39	115.42	586.44	313.74	237.60	47.42	193.86	240.66	90.02
Nb	7.37	4.97	9.53	3.31	5.37	9.88	4.10	9.92	35.95	36.58	23.48	9.54	10.12	11.33	7.87
Cs	1.91	1.81	0.88	0.49	1.17	0.68	1.73	6.06	0.87	3.42	3.04	1.69	0.74	0.55	0.85
Ba	272.27	266.52	683.08	319.26	142.77	454.08	485.45	380.11	331.43	1291.11	758.35	343.75	500.98	569.18	741.30
La	14.52	10.89	30.36	16.97	8.16	7.66	12.89	21.29	78.57	96.12	53.36	14.26	49.66	49.02	16.89
Ce	39.46	31.53	46.96	37.19	28.25	24.97	30.07	50.07	128.34	128.23	76.77	33.19	83.42	58.80	32.95
Pr	5.19	3.89	5.59	4.44	3.58	3.15	3.61	6.55	14.09	16.42	8.98	4.22	9.00	6.35	4.06
Nd	21.43	14.06	20.60	14.83	12.58	8.93	12.06	26.32	59.36	68.59	36.98	17.03	34.65	22.39	14.05
Sm	4.94	2.93	3.39	2.39	3.09	2.14	2.30	5.55	9.59	12.36	6.98	3.76	5.44	3.61	2.76
Eu	1.21	1.15	1.48	1.24	1.44	0.76	0.98	1.03	1.81	2.31	1.84	1.74	1.64	1.33	1.08
Gd	4.67	3.02	2.97	2.29	3.52	3.65	2.31	5.20	6.26	9.49	5.79	3.72	4.21	3.15	2.80
Tb	0.74	0.48	0.42	0.34	0.61	0.73	0.35	0.84	0.80	1.39	0.83	0.56	0.58	0.45	0.43
Dy	4.64	2.48	1.73	1.14	3.98	6.11	1.27	5.52	3.87	8.99	4.81	2.99	2.52	1.90	1.86
Ho	0.97	0.51	0.32	0.20	0.89	1.55	0.22	1.18	0.71	1.78	0.94	0.60	0.42	0.35	0.31
Er	2.61	1.34	0.75	0.43	2.57	4.92	0.47	3.23	1.80	4.68	2.39	1.52	0.85	0.83	0.66
Tm	0.40	0.22	0.11	0.07	0.41	0.81	0.07	0.48	0.27	0.68	0.34	0.22	0.10	0.12	0.10
Yb	2.53	1.42	0.72	0.42	2.69	5.35	0.41	3.03	1.74	4.14	2.11	1.36	0.53	0.77	0.60
Lu	0.39	0.22	0.12	0.07	0.43	0.84	0.06	0.46	0.28	0.59	0.32	0.21	0.08	0.13	0.09
Hf	4.70	3.93	5.87	3.53	3.55	7.52	3.78	3.00	13.35	7.10	5.47	1.04	4.64	5.66	2.78
Ta	0.33	0.24	0.30	0.13	0.33	0.95	0.14	0.46	1.70	1.95	1.11	0.52	0.24	0.43	0.66
Pb	25.10	11.35	13.14	8.57	9.52	13.37	27.94	12.45	10.00	10.34	10.60	11.15	15.76	10.10	12.96
Th	0.70	1.49	0.86	0.64	0.90	7.26	0.64	0.70	10.04	3.50	2.06	0.85	1.06	5.21	5.34
U	0.23	0.38	0.69	0.43	0.75	2.53	0.31	0.20	2.52	1.17	0.92	0.37	0.26	0.90	1.79

Table 6. List of the samples used for geochemical comparison between the Losee Metamorphic Suite, metasedimentary unit, and hypersthene-quartz-oligoclase gneiss. Data for the Losee Suite and metasedimentary rocks from Volkert and Drake (1999).

	Losee Suite	Hypersthene-quartz-oligoclase Gneiss	Metasedimentary Unit
Felsic Samples	471, 472, 638, 23, 56, B1, 141, F1, 175, 104, 994, 279, 345, & 96	BM-6 & BM-13	71, D2, 95, S381, WA200, 426, & 692
Intermediate Samples	28, 36, F79, 46, 94, 128, 7, 275, 3, W66, 255, 435, 664, W284, 423, 639, 527, 138, G37, 275, & 1106	BM-1, BM-2, BM-3, BM-4, BM-5, BM-7, BM-8-M, BM-11, & BM-12	30, 4, 100, WA311, H147, 44, GL13, 299, 260, 121, 384, 259, 1045, & 63
Mafic Samples	114, 561, 43, & H381	BM-8-T, BM-8-B, BM-9, & BM-10	M284 & 242

Table 7. Geochemical comparison of major and select trace elements between the Losee Metamorphic Suite, metasedimentary unit, and hypersthene-quartz-oligoclase gneiss. Data for the Losee Suite and metasedimentary rocks from Volkert and Drake (1999).

Major Element (wt %)	Average Composition of Felsic Samples			Average Composition of Intermediate Samples			Average Composition of Mafic Samples		
	Losee Suite	Hypersthene-quartz oligoclase Gneiss	Metasedimentary Unit	Losee Suite	Hypersthene-quartz oligoclase Gneiss	Metasedimentary Unit	Losee Suite	Hypersthene-quartz oligoclase Gneiss	Metasedimentary Unit
SiO ₂	73.39	74.45	73.19	64.94	63.10	66.13	50.39	49.92	54.70
TiO ₂	0.29	0.33	0.40	0.61	0.69	0.63	0.86	1.75	0.93
Al ₂ O ₃	13.83	13.51	13.03	16.20	17.14	14.40	17.79	17.94	11.30
FeO _{total}	1.90	1.22	2.48	4.33	4.80	4.72	9.31	10.33	8.83
MnO	0.04	0.00	0.06	0.07	0.05	0.09	0.15	0.09	0.15
MgO	0.59	0.78	0.52	1.94	2.18	1.54	6.51	4.49	4.35
CaO	2.39	1.03	1.22	3.82	4.39	3.41	11.17	7.54	14.55
Na ₂ O	5.00	2.85	3.75	4.83	4.01	4.79	2.78	3.46	3.65
K ₂ O	1.94	4.85	4.55	1.88	2.28	3.16	0.44	3.12	0.66
P ₂ O ₅	0.06	0.08	0.16	0.19	0.21	0.19	0.13	0.42	0.39
Trace Element (ppm)	2.58	0.59	0.84	2.96	1.76	1.52	6.32	1.12	5.39
Ba	590.00	477.53	628.33	422.22	363.59	560.00	118.25	693.33	85.00
Sr	343.33	304.16	115.00	318.89	247.38	172.67	555.00	328.79	225.00

Table 8. Geochemical compositions of samples from the Losee Metamorphic Suite chosen for comparison with the hypersthene-quartz-oligoclase gneiss. Y1b is biotite-quartz-oligoclase gneiss. Data provided by (Volkert & Drake, 1999).

Major Element (wt. %)	Losee Metamorphic Suite samples of Felsic Composition														Ave. Comp.
	(Y1a) Quartz-oligoclase Gneiss											(Y1b) Characteristic Rhyolite		(Y1b)	
	471	472	638	23	56	B1	141	F1	175	104	279	345	96	994	
SiO ₂	70.40	75.50	71.40	74.90	71.10	77.20	76.90	73.20	73.20	72.90	73.40	72.90	72.60	71.90	73.39
TiO ₂	0.42	0.24	0.17	0.33	0.44	0.23	0.25	0.15	0.11	0.47	0.30	0.26	0.30	0.36	0.29
Al ₂ O ₃	15.20	12.90	16.40	13.00	15.30	12.20	12.10	15.30	15.60	13.10	13.00	14.20	10.50	14.80	13.83
FeO _{total}	2.29	2.59	1.31	0.80	1.91	1.39	1.27	0.89	0.44	2.34	2.45	2.16	5.14	1.65	1.90
MnO	0.03	0.02	0.06	0.01	0.02	0.03	0.03	0.07	0.01	0.03	0.04	0.04	0.06	0.04	0.04
MgO	1.37	0.38	0.45	0.56	0.71	0.39	0.56	0.29	0.01	0.52	1.15	0.49	0.27	1.10	0.59
CaO	2.21	2.79	4.05	1.16	2.75	2.90	2.80	1.50	1.77	2.79	2.33	2.29	1.15	2.90	2.39
Na ₂ O	5.45	3.97	5.12	6.95	5.19	5.94	6.22	4.70	6.92	5.96	3.92	4.17	1.25	4.30	5.00
K ₂ O	1.98	1.10	0.83	1.54	2.19	0.62	0.53	1.40	1.14	1.21	2.78	3.19	7.49	1.20	1.94
P ₂ O ₅	0.06	0.03	0.06	0.04	0.11	0.04	0.03	0.04	0.03	0.13	0.07	0.07	0.03	0.07	0.06
Na ₂ O/K ₂ O	2.75	3.61	6.17	4.51	2.37	9.58	11.74	3.36	6.07	4.93	1.41	1.31	0.17	3.58	2.58
Trace Element (ppm)															
Ba	390	130	450	290	1000	80	140	-----	1000	260	1200	640	1500	-----	590.00
Sr	450	160	790	80	650	80	120	-----	880	340	240	280	50	-----	343.33

Table 9. Geochemical compositions of samples from the Losee Metamorphic Suite chosen for comparison with the hypersthene-quartz-oligoclase gneiss. Data from (Volkert and Drake, 1999).

Losee Metamorphic Suite Samples of Mafic Composition					
(Yd) Massive Charnockitic Rocks					
Major Element (wt. %)	114	561	43	H381	Avg. Comp.
SiO ₂	50.77	52.40	46.70	51.70	50.39
TiO ₂	1.08	0.26	0.51	1.58	0.86
Al ₂ O ₃	14.26	20.60	21.00	15.30	17.79
FeO _{Total}	12.83	4.84	8.99	10.60	9.31
MnO	0.18	0.09	0.14	0.17	0.15
MgO	6.67	6.43	6.46	6.48	6.51
CaO	10.08	12.50	13.50	8.60	11.17
Na ₂ O	3.40	2.50	1.60	3.60	2.78
K ₂ O	0.38	0.30	0.39	0.70	0.44
P ₂ O ₅	0.13	0.06	0.08	0.26	0.13
Na ₂ O /K ₂ O	8.95	8.33	4.10	5.14	6.63
Trace Element (ppm)					
Ba	53.00	90.00	60.00	270.00	118.25
Sr	180.00	830.00	810.00	400.00	555.00

Table 10. Geochemical compositions of samples from the Losee Metamorphic Suite chosen for comparison with the hypersthene-quartz-glioclase gneiss. Data provided by (Volkert & Drake, 1999).

Major Element (wt %)	Losee Metamorphic Suite Samples of Intermediate Composition										AVE Comp.										
	(Y1b) Biotite-quartz-glioclase Gneiss				(Y10) Quartz-glioclase Gneiss				(Y1b) Charnocitic Dacite												
	435	W66	255	664	W28	423	639	527	36	F79	46	94	128	7	28	275	3	138	G37	275	1106
SiO ₂	69.0	63.3	61.1	61.1	62.50	60.3	61.6	58.4	67.5	69.0	69.8	69.7	65.8	66.6	64.4	64.9	62.9	67.2	66.0	65.3	66.3
TiO ₂	0.53	0.88	0.91	1.02	0.76	1.83	0.71	0.58	0.23	0.20	0.34	0.19	0.51	0.30	0.49	0.45	0.94	0.54	0.62	0.44	0.41
Al ₂ O ₃	15.2	17.0	16.2	13.9	17.30	15.1	14.4	17.2	18.2	17.3	14.8	17.6	16.0	19.0	16.0	16.3	15.6	15.9	15.7	16.1	15.4
FeO _{total}	0	0	0	0	0	0	0	0	0	0	0	0	0	0	0	0	0	0	0	0	0
FeO _{calc}	2.76	3.76	7.05	8.73	2.34	8.64	5.96	8.48	1.58	1.16	2.37	1.30	4.07	1.92	4.14	3.99	5.26	3.52	6.23	4.36	3.42
MnO	0.05	0.02	0.02	0.11	<0.1	0.12	0.09	0.15	0.03	0.03	0.03	0.03	0.07	0.01	0.08	0.07	0.07	0.09	0.11	0.07	0.10
MgO	0.99	3.66	2.99	3.11	3.36	2.09	3.51	3.06	0.88	0.80	0.91	0.66	1.93	0.18	2.02	1.76	2.50	1.32	0.82	1.95	2.20
CaO	3.29	2.66	3.43	3.05	2.19	5.68	5.14	4.82	3.92	4.30	1.09	4.64	4.81	3.44	4.39	4.72	4.16	4.07	3.75	4.75	2.00
Na ₂ O	5.11	6.41	5.48	3.12	6.88	4.07	4.15	4.07	5.62	5.12	4.68	5.1	4.56	6.56	4.68	4.51	4.20	4.17	5.02	4.44	3.50
K ₂ O	2.13	2.05	1.93	2.69	2.10	1.49	1.70	2.29	1.71	1.36	2.70	0.85	1.62	1.43	1.10	1.46	1.30	1.94	1.34	1.51	4.80
P ₂ O ₅	0.15	0.22	0.19	0.22	0.15	0.61	0.22	0.20	0.10	0.10	0.13	0.08	0.18	0.03	0.15	0.18	0.25	0.16	0.21	0.18	0.27
Na ₂ O/ K ₂ O	2.40	3.13	2.84	1.16	3.28	2.73	2.44	1.78	3.29	3.76	1.73	6.00	2.81	4.59	4.25	3.09	3.23	2.15	3.75	2.94	0.73
Trace Elements (ppm)																					
Ba	930	300	670	350	200	860	480	260	450	650	1200	480	410	220	220	460	600	870	420	520	523.68
Sr	590	130	140	80	140	570	370	130	750	1000	510	800	630	130	610	730	500	590	320	750	470.53

Table 11. Geochemical compositions of samples from the metasedimentary rocks chosen for comparison with the hypersthene-quartz-oligoclase gneiss. Data from (Volkert and Drake, 1999).

Metasedimentary Rock Samples of Felsic Composition								
Major Element (wt. %)	(Yb) Biotite-quartz-Feldspar Gneiss		(Ymp) Clinopyroxene-quartz-feldspar Gneiss					Avg.
	71	D2	95	S381	WA200	426	692	
SiO ₂	70.90	76.60	74.50	71.80	73.80	74.30	70.40	73.19
TiO ₂	0.66	0.45	0.28	0.53	0.27	0.33	0.27	0.40
Al ₂ O ₃	13.20	13.10	12.60	12.80	12.50	13.20	13.80	13.03
FeO _{Total}	4.58	1.00	2.24	3.31	2.08	2.19	1.95	2.48
MnO	0.19	0.01	0.03	0.06	0.03	0.02	0.05	0.06
MgO	1.43	0.29	0.27	0.60	0.30	0.39	0.33	0.52
CaO	1.72	0.61	1.23	2.01	1.06	0.43	1.45	1.22
Na ₂ O	2.18	3.40	3.66	4.02	3.86	5.29	3.87	3.75
K ₂ O	4.06	4.20	4.65	4.13	5.41	3.83	5.58	4.55
P ₂ O ₅	0.07	0.02	0.06	0.10	0.05	0.04	0.09	0.06
Na ₂ O/ K ₂ O	0.54	0.81	0.79	0.97	0.71	1.38	0.69	0.84
Trace Element (ppm)								
Ba	790.00	_____	620.00	710.00	340.00	530.00	780.00	628.33
Sr	180.00	_____	90.00	110.00	80.00	50.00	180.00	115.00

Table 12. Geochemical compositions of samples from the Metasedimentary rocks chosen for comparison with the hypersthene-quartz-oligoclase gneiss. Ymp is clinopyroxene-quartz-feldspar gneiss. Data provided by (Volkert & Drake, 1999).

Major Element (wt. %)	Metasedimentary Rock Samples of Intermediate Composition										Avg. Comp.								
	(Ymp) Biotite-quartz-feldspar Gneiss				(Ymh) Hornblende-quartz-feldspar Gneiss				(Yp) Pyroxene Gneiss										
	299	30	44	GL13	WQ311	4	Avg. Comp.	100	WA311	H147	Avg. Comp.	260	63	121	384	259	1045	Avg. Comp.	
SiO ₂	59.40	65.90	66.40	67.60	67.00	67.90	66.96	67.70	68.20	66.10	67.33	59.20	65.40	67.50	67.60	68.20	67.90	65.97	
TiO ₂	1.65	0.72	0.56	0.71	0.67	0.49	0.63	0.57	0.47	0.43	0.49	0.44	0.65	0.73	0.64	0.51	0.16	0.52	
Al ₂ O ₃	14.70	16.10	16.50	13.80	13.70	13.80	14.78	14.90	12.90	14.50	14.10	11.70	14.80	14.00	14.70	13.10	16.80	14.18	
FeO _{total}	8.20	2.67	2.51	4.38	5.74	7.08	4.48	4.59	6.87	6.86	6.11	6.92	4.12	3.62	2.76	3.44	1.10	3.66	
MnO	0.12	0.01	0.02	0.02	0.01	0.17	0.05	0.06	0.11	0.29	0.15	0.06	0.12	0.06	0.15	0.05	0.03	0.08	
MgO	1.62	2.61	2.00	1.86	1.80	1.73	2.00	0.39	0.30	0.22	0.30	3.45	1.42	1.56	1.40	1.98	0.74	1.76	
CaO	4.37	1.66	4.35	2.00	0.66	1.18	1.97	2.87	1.72	1.00	1.86	9.05	5.06	3.87	4.83	5.36	3.10	5.21	
Na ₂ O	4.74	6.37	4.42	3.34	3.76	2.49	4.08	3.47	4.04	2.95	3.49	6.63	6.42	6.20	6.92	5.05	5.00	6.04	
K ₂ O	4.04	3.32	1.66	4.34	5.43	3.84	3.72	4.91	5.06	6.63	5.53	0.70	0.90	0.78	0.31	1.53	3.97	1.37	
P ₂ O ₅	0.48	0.13	0.41	0.18	0.10	0.06	0.18	0.15	0.07	0.04	0.09	0.64	0.16	0.16	0.19	0.02	0.07	0.21	
Na ₂ O/ K ₂ O	1.17	1.92	2.66	0.77	0.69	0.65	1.34	0.71	0.80	0.44	0.65	9.47	7.13	7.95	22.32	3.30	1.26	8.57	
Trace Element (ppm)																			
Ba	1400	440	290	710	610	1200	650.00	1400	410	440	750.00	40	130	290	150	220	670	250.00	
Sr	260	100	390	120	90	100	160.00	310	50	80	146.00	70	260	180	230	180	170	181.67	

Table 13. Geochemical compositions of samples from the Metasedimentary rocks chosen for comparison with the hypersthene-quartz-oligoclase gneiss. Data provided by (Volkert and Drake, 1999).

Metasedimentary Rock Samples of Mafic Composition			
(Yp) Pyroxene Gneiss			
Major Element (wt. %)	M284	242	Avg. Comp.
SiO ₂	50.28	56.60	54.70
TiO ₂	0.87	0.99	0.93
Al ₂ O ₃	11.80	10.80	11.30
FeO _{Total}	9.57	8.10	8.83
MnO	0.19	0.11	0.15
MgO	3.61	5.09	4.35
CaO	18.30	10.80	14.55
Na ₂ O	1.90	5.39	3.65
K ₂ O	0.79	0.52	0.66
P ₂ O ₅	0.14	0.63	0.39
Na ₂ O /K ₂ O	2.41	10.37	6.39
Trace Element (ppm)			
Ba	40.00	1300.00	85.00
Sr	380.00	70.00	225.00

Table 14. Average geochemical compositions of units from the Loose Metamorphic Suite and Metasedimentary rocks chosen for comparison with the hypersthene-quartz-oligoclase gneiss. Ymp values represent a single sample, not an average. Yh₁ is charnockitic andesite, Yh₂ is charnockitic dacite. Unit names for the abbreviations listed are given in Tables 8-13. Data provided by (Volkert & Drake, 1999).

Major Element (wt %)	Loose Metamorphic Suite				Hypersthene-quartz-oligoclase Gneiss	Metasedimentary Rocks			
	Yhb	Yh ₁	Yh ₂	Yh ₃		Ymp	Yb	Ymh	Yp
SiO ₂	63.60	60.10	66.73	66.20	63.10	59.40	66.96	67.33	65.97
TiO ₂	0.82	1.04	0.41	0.50	0.69	1.65	0.63	0.49	0.52
Al ₂ O ₃	15.92	15.57	16.76	15.78	17.14	14.70	14.78	14.10	14.18
FeO _{Total}	4.97	7.49	2.89	4.38	4.80	8.20	4.48	6.11	3.66
MnO	0.05	0.12	0.05	0.09	0.05	0.12	0.05	0.15	0.08
MgO	2.82	2.89	1.29	1.57	2.18	1.62	2.00	0.30	1.76
CaO	2.92	5.21	3.94	3.64	4.39	4.37	1.97	1.86	5.21
Na ₂ O	5.40	4.10	5.00	4.28	4.01	4.74	4.08	3.49	6.04
K ₂ O	2.18	1.83	1.50	2.40	2.28	4.04	3.72	5.53	1.37
P ₂ O ₅	0.19	0.34	0.13	0.21	0.21	0.48	0.18	0.09	0.21
Na ₂ O/ K ₂ O	2.56	2.32	3.64	2.39	1.76	1.17	1.34	0.65	8.57
Trace Elements (ppm)									
Ba	490.00	533.33	511.25	603.33	363.59	1400.00	650.00	750.00	250.00
Sr	216.00	346.67	645.00	553.33	247.38	260.00	160.00	146.67	181.67

Table 15. Standard deviations of the average geochemical compositions of units from the Losee Metamorphic Suite and Metasedimentary rocks chosen for comparison with the hypersthene-quartz-oligoclase gneiss. Yh₁ is charnockitic andesite, Yh₂ is charnickitic dacite. Unit names for the abbreviations listed are given in Tables 8-13. Data provided by (Volkert & Drake, 1999).

Major Element (wt. %)	Losee Metamorphic Suite				Hypersthene-quartz-oligoclase Gneiss	Metasedimentary Rocks		
	Ylb	Yh ₁	Ylo	Yh ₂		Yb	Ymh	Yp
SiO ₂	3.12	1.61	2.46	0.79	3.43	0.83	1.10	3.46
TiO ₂	0.19	0.69	0.23	0.10	0.18	0.10	0.07	0.21
Al ₂ O ₃	1.39	1.46	1.35	0.30	1.01	1.40	1.06	1.72
FeO ^{total}	2.77	1.35	1.50	1.30	1.59	1.97	1.31	1.91
MnO	0.04	0.03	0.03	0.02	0.05	0.07	0.12	0.05
MgO	1.06	0.73	0.78	0.62	0.97	0.36	0.09	0.92
CaO	0.50	0.43	1.15	1.17	1.56	1.42	0.94	2.06
Na ₂ O	1.46	0.05	0.72	0.63	0.50	1.46	0.55	0.82
K ₂ O	0.30	0.41	0.52	1.62	1.04	1.39	0.95	1.34
P ₂ O ₅	0.04	0.23	0.07	0.05	0.05	0.14	0.06	0.22
Na ₂ O/ K ₂ O	0.85	0.49	1.21	1.29	0.76	0.91	0.18	7.40
Trace Elements (ppm)								
Ba	302.41	303.53	311.88	236.29	170.50	346.91	563.12	222.44
Sr	210.55	211.27	254.45	217.33	135.00	129.03	142.24	64.94

Table 16. Normalization values used for producing REE plots and multi-element plots. Sample values were normalized to 1. Chondrite normalization factors from Masuda *et al.* (1973). N-MORB normalization factors from Sun and McDonough (1989).

Element	Chondrite	N-MORB
K	-----	581
Ti	-----	7614
Nb	-----	2.33
Rb	-----	0.56
Sr	-----	135
Cs	-----	0.007
Ba	-----	6.30
La	0.3780	
Ce	0.9760	7.50
Pr	0.5100	-----
Nd	0.7160	7.30
Sm	0.2300	2.63
Eu	0.0866	1.02
Gd	0.3110	-----
Tb	0.0589	0.67
Dy	0.3900	-----
Ho	0.0872	-----
Er	0.2550	-----
Tm	0.0393	-----
Yb	0.2490	3.05
Lu	0.0387	0.85
Hf	-----	2.05
Ta	-----	0.132
Th	-----	0.12
U	-----	0.047